Continuous microaeration of mesophilic anaerobic digestion for *in situ* biogas desulfurization

by

MANAV BAID

A thesis submitted in partial fulfillment of

the requirements for the degree of

Master of Science

(Civil and Environmental Engineering)

at the

UNIVERSITY OF WISCONSIN-MADISON

2024

Date of Final Oral Exam: 11/22/2024

The thesis is approved by the following members of the final oral committee:
Daniel R Noguera, Professor, Civil and Environmental Engineering
Katherine D. McMahon, Professor, Civil and Environmental Engineering and Bacteriology
Matt Seib, PhD, PE, Assistant Operations Manager, Madison Metropolitan Sewerage District

TABLE OF CONTENTS

ACKNOWLEDGMENTS

This thesis was a result of the work by many individuals and institutions. Firstly, I would like to extend my gratitude to Prof. Daniel R Noguera for his relentless and unabating support and guidance – I could not have wished for a better mentor to help me learn how to not only perform uncompromising research but also function more efficiently in every part of my life. Few have had a chance to intentionally add oxygen to an anerobic digester and I am grateful for this opportunity. I would also like to thank Dr. Matt Seib at the Madison Metropolitan Sewerage District for his valuable support and insights throughout the two years of my tenure. I thank Prof. Trina McMahon for her support as part of my thesis committee.

This research was conducted with the help of various people who helped me ensure the bioreactors ran as well as they did; I acknowledge the assistance of Brayan Daniel Riascos Arteaga, Lillian Glackin, Anna Schoessor, Nina T Pfeiffer, and Lily Schick towards daily operation of the bioreactors. I would like to thank Jackie Bastyr Cooper for assistance with procurement of the materials required for conducting the study as well as for training me on using the GCs. I would like to thank Dr Rachelle A. Stenzel Lemke for helping me setup the lab space. I would like to give a special thanks to Dr. Bumkyu Kim and Brayan Riascos for their assistance in cleaning up the lab space at the end of the period of operation of the bioreactors. I also extend my gratitude to all the members of the Noguera-Donohue lab at the University of Wisconsin-Madison, whom I had the pleasure to meet throughout my tenure, for their vital support.

I thank the Madison Metropolitan Sewerage District, for their funding support towards this research and my education, the Wisconsin Energy Institute at UW-Madison, for providing me with the lab space to conduct this research, and the Department of Civil and Environmental Engineering, College of Engineering, UW–Madison, for giving me a chance of a lifetime.

I also extend my gratitude to all my family and friends, both old and those I made during my time in Madison, for their friendship and support. Shoutout to all my housemates at International Cooperative House, it was never a dull moment living there. Special thanks to Anupreksha Jain for her patience and companionship. Lastly, I extend my unending gratitude to Mummy, Papa, and Bhaiya, for being my anchor in this storm – I love you and I have missed you all dearly.

ABSTRACT

Anaerobic digestion can be vital in helping water resource recovery facilities improve their renewable energy portfolio through the generation of methane-rich biogas. The biogas must be stripped of various trace components such as hydrogen sulfide (H_2S) before reuse to maintaining the operation life of the machinery. Microaeration, which is the addition of trace amounts of oxygen or air, has been demonstrated to be an effective low-cost method for *in situ* biogas desulfurization in single stage anaerobic digesters. There is further evidence that suggests that microaeration aids hydrolysis, thereby improving solids destruction. This study aimed to understand the efficacy of continuous microaeration, using bubble-free supply of oxygen into the sludge recirculation line, in the methanogenic stage of a mesophilic two-stage anaerobic digestion process for biogas desulfurization and for improving solids destruction. The doses tested in this investigation were 0.0, 0.67, 5.35, 7.50, and 15.0 $mL_{O2}/L_{reactor}$–day.

Microaeration led to a decrease in the H_2S from 750 $\pm$ 120 ppm at a microaeration dose of 0.0 $mL_{O2}/L_{reactor}$–day, i.e., when completely anaerobic, to 220 $\pm$ 80 ppm at 15.0 $mL_{O2}/L_{reactor}$–day in the Experimental bioreactor. There was no significant change in the volatile solids destruction efficiency across the different doses of microaeration, suggesting that, up to a dose 15.0 $mL_{O2}/L_{reactor}$–day, microaeration does not impact solids destruction. There was an increase in the methane fraction in the biogas, from 64.4 $\pm$ 2.0% at 7.50 $mL_{O2}/L_{reactor}$–day to 65.7 $\pm$ 1.6% at 15.0 $mL_{O2}/L_{reactor}$–day, while CO_2 reduced from 34.3 $\pm$ 1.3% during the same period to 29.7 $\pm$ 0.9%. Methane yield was consistent almost throughout the operation period, at 0.75 $\pm$ 0.03 L_{CH4}/g_{VS} in the Experimental

bioreactor compared to 0.67 ± 0.04 L_{CH4}/g_{VS} in the Control bioreactor.

This study validated that continuous microaeration can be used for *in situ* biogas desulfurization in the methanogenic stage of a mesophilic two-stage anaerobic digestion process, without any significant adverse effect to the anaerobic community.

LIST OF FIGURES

LIST OF TABLES

This page left intentionally blank

INTRODUCTION

Anaerobic digestion

The United Nations Conference of Parties (COP), in its 28th Annual Meeting, acknowledged the detrimental effect of the use of fossil fuels towards global warming, and promoted the use of renewable energy as a crucial step for climate action (Sanderson, 2023). Globally, the water resource recovery sector is responsible for consumption of about 4% of the total energy output (IEA, 2018). Anaerobic digestion (AD) is a powerful technology for veritable non-fossil-fuelled, bio-based production of fertilizer and renewable energy through the production of biogas as a gaseous fuel (Tessele and van Lier, 2020). With a long history of industrial implementation, anaerobic digestion has demonstrated its versatility in terms of the feedstocks that this process can treat to produce methane-rich biogas. In municipal sanitation, anaerobic digestion has found a wide range of applications in centralized and de-centralized wastewater management and pollution control, from septic tanks for small and localized fecal sludge management to anaerobic digesters used for biosolid handling in large water and resource recovery facilities (WRRFs) that handle hundreds of millions of gallons of wastewater per day (Almansa et al., 2023). In recent years, AD has indicated immense potential as a means of recovering resources in the form of energy and value-added products and promoting the water resource recovery sector as a potential player towards developing a more circular economy (Tessele and van Lier, 2020).

Anaerobic digestion is a biochemical process that can be summarized as the gradual breakdown of complex organic substrates into mineralized products, such as methane (CH_4), carbon dioxide (CO_2), ammonia (NH_3), and hydrogen sulfide (H_2S), by the concerted action of a consortium consisting of several groups of microorganisms under anaerobic conditions.

Methane production in the AD process may follow one of many pathways (Figure 1). Following hydrolysis and fermentation by fermentative microorganisms, the ethanol and VFAs produced are converted to primarily acetic acid, H_2 and CO_2 by hydrogen-producing acetogenic microorganisms, in a step called acetogenesis. These can be consumed to produce CH_4 via multiple pathways, and this step is called methanogenesis. The acetic acid can be directly consumed to produce CH_4 and CO_2, and this pathway is called acetoclastic methanogenesis; the H_2 and CO_2 can be utilized by one of two pathways — direct conversion to CH_4, which is called hydrogenotrophic methanogenesis or conversion to acetic acid in a step called homoacetogenesis, which then follows acetoclastic methanogenesis. Acetogenesis is regarded thermodynamically favorable only when the partial pressure of H_2 is above 10^{-3} atm. This condition is fulfilled by the H_2—scavenging microorganisms present such as the homoacetogens and the hydrogenotrophic methanogens (Khanal, 2008).

Anaerobic digestion of municipal sludge is an attractive technology for reducing carbon emissions at WRRFs since the biogas produced can be used for energy generation thus providing WRRFs with an opportunity to reduce the purchase of fossil-fuel derived electricity and heat to satisfy their energy requirements. This makes AD a key channel for alleviating the reliance of WRRFs on energy grids and improve their renewable energy portfolio.

The primary components of the biogas produced during the anaerobic digestion process are CH_4 (55%-65%) and CO_2 (35%-44%) (Rasi et al., 2011). Some of the other gases found in trace quantities are water vapor, H_2S, volatile organic carbon compounds, and siloxanes (Rasi et al., 2011). Thus, while being a rich source of methane, the biogas requires downstream treatment for the removal of H_2S and siloxanes, and depending on the

downstream use, the removal of CO_2 (Rasi et al., 2011).

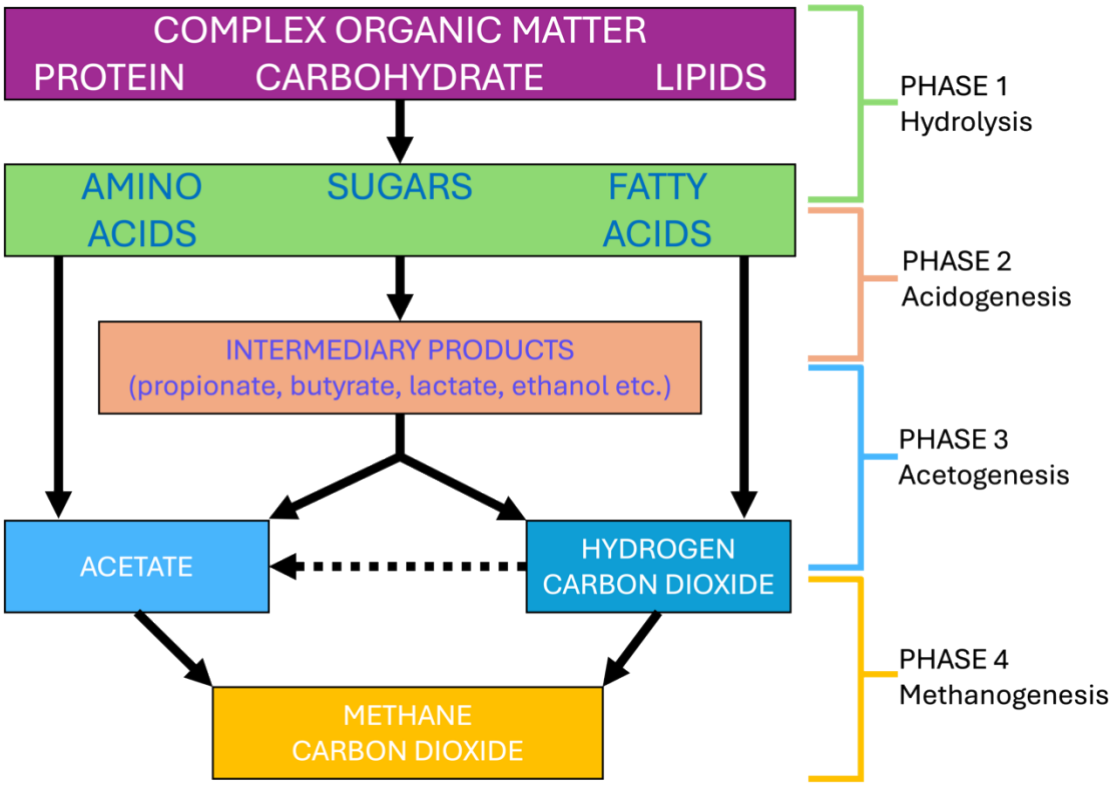

Figure 1. Conversion steps in anaerobic digestion of complex organic matter. Adapted from (Khanal, 2008).

Hydrogen sulfide in anaerobic digestion

Sulphur is present in all biological materials and especially in those containing high concentrations of proteins. Methionine and cysteine are common sulfur-containing amino acids in proteins. In anaerobic processes, H_2S and other sulfide compounds originate from these organic sources as well as from the biological reduction of inorganic forms of sulfur, such as sulfate (SO_4^{2-}) (Vu et al., 2022). H_2S concentrations in the biogas greatly vary; the usual reported values are about 1000 ppm but the concentrations as high as 10000 ppm have also been reported in literature (Rasi et al., 2011).

Even in trace amounts it has a pertinent and detrimental impact on the potential of

biogas use. H_2S conversion to sulfur oxides (SO_x) and sulfuric acid (H_2SO_4) during biogas combustion results in severe corrosion of the piping system and other industrial installations (Giordano et al., 2019). Thus, H_2S levels in biogas should not exceed 1000 ppm if traditional boilers and internal combustion engines are utilized for electricity generation and even stricter limits (<0.1 ppm) are required for off-site biogas utilization, e.g. as vehicle fuel or in fuel cells (Rasi et al., 2011). Furthermore, dissolved H_2S concentrations over 50 mg/L, in the sludge, have been reported to be inhibitory to activity of the methanogens in the AD system (Oude Elferink et al., 1994). Current in situ methods for the removal of H_2S include addition of chemicals such as ferric chloride for the removal. However, and chemical production typically has a large impact on the environment, thus creating the need for a low-impact, chemical-free method for in situ removal of H_2S (Azizi et al., 2023).

Microaeration

Microaeration of anaerobic digestion is the addition of trace amounts of air or oxygen to the anaerobic digester. While oxygen (O_2) strongly inhibits the growth and metabolism of obligate anaerobic microorganisms, especially methanogens, exposure to oxygen is inevitable in practical applications. Early investigations on the effect of oxygen exposure on methanogenesis in granular anaerobic sludge showed that methanogens exhibited some tolerance towards oxygen exposure (Fu et al., 2023). Furthermore, existing literature on single stage anaerobic digesters suggests that microaeration could lead to nearly 100% reduction of H_2S in the biogas produced during anaerobic digestion, compared to pre-microaerated conditions (Giordano et al., 2019). The reported maximum H_2S removal from the biogas has ranged from 68% to >99% in single stage AD systems (Krayzelova et al., 2015).

There has been evidence of microaeration in single stage AD systems improving the destruction of solids in the process leading to greater reduction in sludge volume (Chen et al., 2020; Fu et al., 2023; Nguyen and Khanal, 2018). The proposed mechanism is that addition of oxygen facilitates the growth and metabolism of facultative hydrolytic bacteria, accelerating hydrolysis in the AD system (Chen et al., 2020; Fu et al., 2023; Nguyen and Khanal, 2018). However, these observations vary across different studies. It has been suggested that the rate or dose of microaeration affects the outcome on the different performance parameters of and AD system, such as solids destruction, methane yield, and H_2S removal from the biogas (Nguyen and Khanal, 2018).

This study aims at evaluating microaeration as an emerging approach to reduce H_2S in the anaerobic digestion biogas, in the context of the WRRF in Madison, Wisconsin.

Overview of the anaerobic digestion process at the Nine Springs WRRF

The Madison Metropolitan Sewerage District (MMSD) handles the wastewater discharged in the Madison Metropolitan Area at their Nine Springs WRRF (Figure 2). The Nine Springs WRRF operates a two-phase anaerobic digestion process that treats combined thickened primary sludge (PS) and waste activated sludge (WAS). The methanogenic digester has a retention time of 25 days and operates at 35°C. The sludge is mixed through draft tube mixers and heated using heat exchangers along the sludge recirculation line. Ferric chloride is added in this stage to reduce the H_2S loading in the biogas treatment process that follows and sequester phosphorus released during digestion.

Figure 2. Aerial image of the Nine Springs WRRF, operated by Madison Metropolitan Sewerage District. (Picture courtesy: Madison Metropolitan Sewerage District).

Research objectives

The objective of this research was to investigate, at the bench-scale, the impact of microaeration in the methanogenic phase of the two-phase anaerobic digestion process at the Nine Springs WRRF. A control bioreactor (CB) and an experimental bioreactor (EB) were set up i=to simulate the operational conditions of the methanogenic phase anaerobic digester at the Nine Springs WRRF. To simulate microaeration, four different doses of oxygen were delivered to the experimental reactor by using a sludge recirculation line and adjusting the length and type of tubing used in the recirculation line to allow for different oxygen diffusion rates. Routine chemical analyses of the influent, effluent, and biogas streams were performed to monitor the impact of microaeration.

This experimental study sought to test two different hypotheses. First, it was hypothesized that microaeration would improve the solids destruction efficiency in the methanogenic stage of a mesophilic two-phase anaerobic digestion process.

The second hypothesis was that microaeration in the methanogenic phase of a mesophilic two-phase anaerobic digestion process would reduce the concentration of H_2S in the biogas produced in the digester.

Thus far, most studies on the effect of microaeration in anaerobic digestion systems have focused on the effect of microaeration on single-stage processes (Chen et al., 2020; Fu et al., 2023). Only one study of microaeration in a two-phase anaerobic digestion process was found, where the impact microaeration was tested on the first stage of a two-phase anaerobic digester treating food waste (Xu et al., 2014). Therefore, there is a gap of knowledge on whether the same effects would be observed in the methanogenic stage of a two-stage AD process.

MATERIALS AND METHODS

Bench-Scale Reactor Set-up and Experimental Design

Bench-scale bioreactors were used to simulate the methanogenic stage of the Nine Springs anaerobic digestion process (Figure 2). One bioreactor was set up as a control system (CB) that simulated the operational conditions of the Nine Springs process, except for the addition of ferric chloride, which was not implemented at bench-scale. The other bioreactor (EB) was set up as the experimental system that simulated the controlled addition of oxygen into the methanogenic stage, implemented by the addition of an external sludge recirculation line that allowed oxygen to diffuse from the atmosphere into the bioreactor system (Figure 2).

The bench-scale systems used 3-liter glass vessels with overhead mechanical stirrers (Applikon, Getinge, Sweden) and were operated in chemostat conditions with 2-liter working volumes (Figure 3).

The temperature inside the bioreactors was maintained at 35°C using heating blankets connected to Applikon ez-control bioreactor controllers (Getinge, Sweden), which were also used for on-line pH monitoring and controlling the mechanical stirrer, set at 750 revolutions per minute (rpm). As a containment strategy to prevent gas leaks to the laboratory environment, both bioreactors were set up inside a fume hood maintained at ambient temperature and pressure (20°C and 1 atm, respectively).

The bioreactors were inoculated, on April 12th, 2023, with 2 liters of digestate collected from one of the full-scale methanogenic phase digesters at the Nine Springs WRRF. To maintain a 25-day SRT, 80 mL of the bioreactor contents were replaced daily with new feedstock.

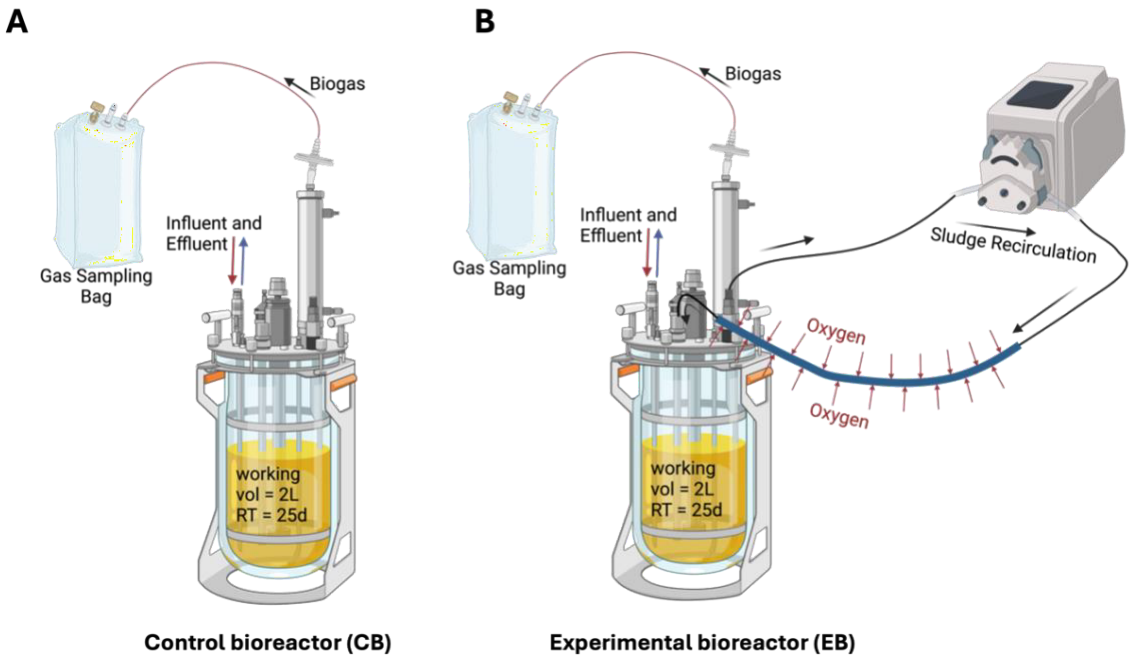

Figure 3. Schematic of bench-scale methanogenic reactors used in this research. (A) The control bioreactor (CB) consisted of a chemostat vessel with port for influent addition and effluent withdrawal and a biogas collection system. (B) The experimental bioreactor (EB) had an additional sludge recirculation line that allowed oxygen to diffuse into the bioreactor through gas permeable tubing.

During operation, 80-mL of bioreactor sludge was extracted daily using a 100-mL syringe (WUSA/100, Wilburn Medical USA). This effluent extraction used a sampling port available at the headplate of the reactor vessels and connected to a stainless-steel tubing that extended to halfway in the sludge blanket. This effluent was used for chemical analyses.

Following effluent collection, the same sampling port was used to inject 80 mL of influent feedstock using a 100-mL syringe. This feedstock was digestate from the Nine Springs' acid-phase anaerobic digesters. The feedstock was collected and transported to the laboratory two times per week, where it was stored at 4°C, and used for up to 4 days of operation.

The biogas produced was collected in Tedlar gas bags of 3-liter capacity and equipped

with a polypropylene valve, and septum fitting (Restek 22051, Restek Corporation, Centre County, PA). Gas accumulation in the bags was measured by either liquid displacement or using a respirometer (AER 800 Research Respirometer, Challenge Technology, USA).

Microaeration

Microaeration of anaerobic digestion is the addition of trace quantities of oxygen or air inside the anaerobic digester. For an anaerobic digester of 3 liter volume, this could imply very low rates of oxygen or air that must be delivered to the digester, usually in terms of 10-100 mL/day. The use of tubing with high gas-permeability to allow bubble-free supply of oxygen into the reactor has been previously demonstrated as a viable method of continuous delivery of oxygen (Li et al., 2023). Thus, bubble-free supply of oxygen using gas-permeable tubing in the recirculation line was used here to microaerate the Experimental bioreactor.

The difference in partial pressure of oxygen inside the anaerobic environment of the reactor and the ambient air allowed for the establishment of a pressure gradient across the tubing walls. Thus, the walls of the tube acted as a membrane with a specific gas permeability and allowed for the diffusion of oxygen. The recirculation line was designed based on Fick's law of diffusion (Hoque and Paul, 2022), which provided a relation between the rate of diffusion of oxygen and the length of gas permeable tubing used.

The rate of gas diffusion through the tubing was estimated using Equation 1, where r is the specific rate of gas diffusion at STP [$mL_{STP}.L_{reactor}^{-1}.day^{-1}$], a is the specific surface area of permeable surface per bioreactor volume [$cm^2.L_{reactor}^{-1}$], l is the length of tubing [cm], Δp is the partial pressure difference [atm], δ is the tubing thickness [cm], and k is the tubing permeability [$mL_{STP}.cm^{-1}.day^{-1}.atm^{-1}$]. The speed of the pump used for sludge recirculation was fixed throughout the duration of the experiments, and it was assumed to be sufficiently

high to carry any diffused oxygen into the reactor vessel.

$$r = \frac{k \times a \times l \times \Delta p}{\delta} \quad (1)$$

For estimating the oxygen permeability (r) using Equation 1, it was assumed that the partial pressure of oxygen inside the tubing was zero and outside the tubing was 0.21 atm. Different combinations of l and k were used to achieve different oxygen dosages in the recirculation line; commercially available tubing with known inner and outer diameters and known specific permeability for oxygen was used. Specifically, two distinct types of tubing – Masterflex L/S 25 Platinum-cured Silicone (VWR) and Masterflex L/S 25 C-FLEX Ultra (VWR) – were chosen (Table 1) and combined at different lengths to obtain the desired oxygen input rates (Table 2).

Table 1. Properties of high gas-permeability tubing used for the recirculation line

	Masterflex L/S 25 Platinum-cured Silicone	**Masterflex L/S 25 C-FLEX Ultra**
Listed permeability (k)	7.961×10^{-7}	1.49×10^{-7}
Calculated k (units change)	0.523	0.013
Inner diameter	0.1875 inches	0.1875 inches
Outer diameter	0.3125 inches	0.3125 inches
Calculated thickness (δ)	0.3175 cm	0.3175 cm

Four different doses of oxygen were chosen (D1 to D4) for introducing microaerobic conditions inside the experimental reactor (Table 2). For each condition, the experimental reactor was operated for a time interval which was equal to three times the SRT, i.e., 75 days, to simulate long term operation, and allow the reactor to reach a steady state (Smith et al., 2018). In addition, preliminary testing of oxygen diffusion was done at two different conditions (P1 and P2 in Table 2), which corresponded to higher diffusion rates than that D1

to D4 testing conditions.

Table 2 Oxygen doses used tested in this bench scale investigation

Experiment no.	Masterflex L/S 25 C-FLEX Ultra		Masterflex L/S 25 Pt-Cured Silicone		Total oxygen diffusion rate ($mL_{STP}.L^{-1}.day^{-1}$)
	Length (cm)	Oxygen diffusion rate ($mL_{STP}.L^{-1}.day^{-1}$)	Length (cm)	Oxygen diffusion rate ($mL_{STP}.L^{-1}.day^{-1}$)	
P1	-	-	127.3	54.6	54.6
P2	32.1	0.34	95.3	40.8	41.2
D1	117.8	1.26	9.50	4.08	5.35
D2	62.9	0.67	0.00	0.00	0.67
D3	48.9	0.53	16.3	6.97	7.50
D4	48.9	0.52	33.8	14.5	15.0

Analytical Methods

The laboratory at MMSD contributed to this research by measuring total solids (TS), volatile solids (VS), and total sulfur. TS and VS were measured using APHA Standard Methods' Method 2540 (American Public Health Association, 1997). Total sulfur in the feedstock and the bioreactor effluents was measured using US EPA Method SW-846 for acid digestion of sludge (EPA, 1996) followed by US EPA Method 200.7, Revision 4.4 for analysis (EPA, 1994).

Volatile fatty acids (VFAs) were measured on filtered samples using a gas chromatograph coupled with a Flame ionization detector (FID) with an autosampler (GC2030, Shimadzu Co., Kyoto Japan), equipped with an autosampler (AOC-6000 Plus, Shimadzu Co., Kyoto, Japan), based on the method described elsewhere (Ingle et al., 2021). The GC used a high–performance capillary column with dimensions of 30m x 0.53mm x 1.00µm (Zebron ZB-FFAP, Phenomenex, Torrance, CA) for underivatized acids and alcohols. Calibration curves for acetic acid, propionic acid, n-butyric acid, isobutyric acid, n-valeric

acid, isovaleric acid, caproic acid, isocaproic acid, and heptanoic acid were prepared using a commercially available standard (Supelco, Sigma-Alrich, USA). The samples for measuring VFAs were filtered through a membrane filter with pore size of 0.45 μm (ThermoFisher Scientific, Waltham, MA, United States). The samples were diluted to half with a 3-molar solution of orthophosphoric acid.

The biogas that was produced was collected in a Tedlar gas bag of 3 liter capacity that was connected to the headplate of the reactor vessel using gas impermeable tubing. The biogas was collected between successive feeding periods which were 24 hours apart. From the beginning of the reactor operation on May 15th, 2023, until October 19th, 2023, following the composition analyses, the volume of biogas produced was measured using a liquid-displacement method; the gas bags were connected to an inverted column of water in a 2-liter graduated cylinder. Pressure would be applied on the gas bag, manually, to deflate the gas bags and measure the volume of water displaced in the measuring cylinder. Starting from October 20th, 2023, the volume of biogas produced was measured online using an AER 800 Research Respirometer (Challenge Technology, USA) that was connected to the gas outlet at the headplate of the reactor vessels. The respirometers were then connected to gas bags, which were later used for composition analyses. The respirometer was filled with an inert liquid in a U-shaped column, which would allow bubbles to form as the gas passed through it before entering the gas bags. An infrared sensor in the device would then count the number of bubbles formed and allow precise online measurement of the biogas produced in the bioreactors. The device was calibrated to estimate the volume corresponding to each bubble of gas passing through the sensor.

CH_4 in the biogas was measured daily using a gas chromatograph (GC) coupled with

a flame ionization detector (FID) (Shimadzu GC2010, Shimadzu Co., Kyoto, Japan) and an AOC20i autosampler (Shimadzu Co, Kyoto, Japan). Helium was the carrier gas. Starting from January 3rd, 2024, the composition of the biogas was measured using MRU Optimax (MRU instruments, USA), a portable gas monitor that measured CH_4, CO_2, O_2, and H_2S in the biogas collected in the gas bags. Approximately 750 mL of biogas was needed for these measurements.

H_2S in the biogas collected was measured daily using a portable handheld gas monitor (Acrulog 1-1000 PPM gas monitor, Analog Instruments, USA). As this device is intended for measurements of H_2S in ambient air, its sensor requires the presence of oxygen in the gas. Since the collected biogas does not contain oxygen, a dilution chamber of known volume was attached to the instrument to enable dilution of the biogas from each gas bag in precise ratios for accurate measurement (Figure 4). The chamber was constructed out of rubber and polyvinyl chloride. The chamber was flushed to zero reading with compressed air before and after each measurement, and 50 mL of the biogas from the gas bags was injected using a 60-mL syringe (Fisherbrand 14955461, ThermoFisher Scientific, Waltham, MA, United States).

Starting from January 3rd, 2024, alongside the Acrulog device, MRU Optimax was also used to measure the concentration of H_2S in the biogas collected in the gas bags.

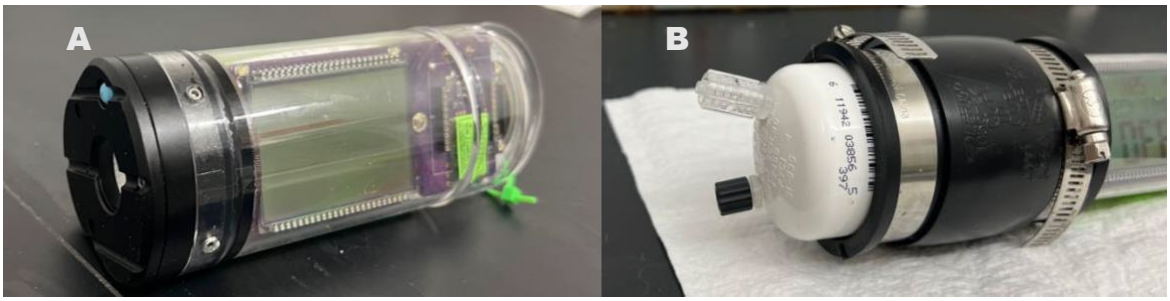

Figure 4. (A) Acrulog PM1000 handheld H2S gas detector. (B) The chamber attached to the handheld device for analyzing biogas collected in gas sampling bags. This chamber had a volume of 235mL and was constructed during this investigation using a rubber tube and PVC tube. The

fittings used for gas exchange are all Luer Lok fittings allowing the use of commercially available syringes for gas exchange.

The temperature and pH were monitored online with the ez-control tower.

Data Analysis

Solids Destruction. Solids destruction in the anaerobic digesters was calculated based on the measured concentration of TS and VS in the feed and in the effluent. The MMSD laboratory provided TS and VS concentrations in weight percentage units. These concentrations can be used to calculate the efficiency of solids destruction in the digester, using Equations 2 and 3, for TS and VS, respectively. These calculations assume that the specific gravity of both the feed and the effluent sludges is equal.

$$\text{TS destruction efficiency } (\%) = \{\, 1 - \frac{\text{TSeffluent}}{\text{TSfeed}} \} * 100 \quad (2)$$

$$\text{VS destruction efficiency } (\%) = \{\, 1 - \frac{\text{VSeffluent}}{\text{VSfeed}} \} * 100 \quad (3)$$

Methane Yield. The yield of methane gas through the chemical oxygen demand (COD) removed was calculated to understand the impact of microaeration on methane yield, Y_{CH4}.

For this, the concentration of VS in the feed and the effluent was first converted to metric units using Equations 4 and 5, respectively. The volumes of biogas and methane here were reported for 20°C and 1 atm. For calculating the concentration of VS in the feed and the effluent, the specific gravity of both the feed and the effluent was assumed to be 1.0, and thus, the density of both the sludges was 1 g_{VS}/L. Those concentrations were then used to calculate the VS removal rate using mass balance from Equation 6. The flow rates of feed and effluent were fixed at 0.08 L/day for both.

$$C_{VS_{feed}} \left(\frac{g_{VS}}{L_{feed}}\right) = \%VS \left(\frac{g_{VS}}{g_{feed}}\right) \times \text{density of feed sludge} \left(\frac{g_{feed}}{L_{feed}}\right) \quad (4)$$

$$C_{VS_{eff}}\left(\frac{g_{VS}}{L_{feed}}\right) = \%VS\ \left(\frac{g_{VS}}{g_{eff}}\right) \times \text{density of effluent}\left(\frac{g_{eff}}{L_{eff}}\right) \quad (5)$$

$$\text{VS Removal Rate}\ \left(\frac{g_{VS}}{day}\right) = C_{VS_{feed}}\left(\frac{g_{VS}}{L_{feed}}\right) \times Q_{in}\left(\frac{L_{feed}}{day}\right) - C_{VS_{eff}}\left(\frac{g_{VS}}{L_{eff}}\right) \times Q_{eff}\left(\frac{L_{eff}}{day}\right). \quad (6)$$

From the biogas production rate, and the concentration of CH_4 from gas composition analyses, the methane production rate was estimated using Equation 7. Finally, the results were applied to Equation 8 to estimate the value of Y_{CH4}.

$$\text{Methane Production Rate}\ \left(\frac{L_{CH_4}}{day}\right) = \text{Biogas Production Rate}\ \left(\frac{L_{Biogas}}{day}\right) \times \%\ \frac{V_{CH_4}}{V_{Biogas}} \quad (7)$$

$$\text{Methane Yield, } Y_{CH_4}\left(\frac{L_{CH_4}}{g_{VS}}\right) = \frac{\text{Methane Production Rate}\ \left(\frac{L_{CH_4}}{day}\right)}{\text{VS Removal Rate}\ \left(\frac{g_{VS}}{day}\right)} \quad (8)$$

Statistical analyses. Comparisons across oxygen doses in the experimental bioreactor and between the control and experimental bioreactors were conducted using unpaired two-sided Welch's t-tests with the cutoff set at 95% confidence level (p-value = 0.05). These tests were performed using Microsoft Office Excel 2016.

RESULTS

The effect of adding small amounts of air to the methanogenic phase of the anaerobic digestion system was evaluated in bench-scale reactors that were operated simulating the operational conditions of the full-scale methanogenic phase digester at the Nine Springs WRRF. To accomplish this simulation, the following operational conditions were implemented:

- The reactor was seeded with anaerobic digestion sludge from the full-scale bioreactor.
- The reactor was fed with the effluent of the acid-phase digester at the full-scale facility, to account for real-world variability in the composition of the feedstock.
- The temperature was maintained at 35°C via online temperature monitoring coupled with a PID-controller equipped-heating blanket.
- The reactor was continuously mixed at 750 rpm.
- The reactor was fed 80 mL of acid-phase sludge daily and the same volume was removed from the reactor prior to feeding. With a working volume of 2.0 L, this operation kept the solids and hydraulic retention times at 25 days.
- Each dose of air delivery was maintained for three times the residence time to simulate long-term operation of the AD system.

One bioreactor was used as a control bioreactor (Figure 2) and operated as indicated above. The main difference with respect to the operation of the full-scale system is that the bench-scale bioreactors did not receive ferric chloride, which in the full-scale system serves the dual purpose of controlling H_2S in the biogas and reducing the concentration of orthophosphate in the liquid digestate. A second bioreactor was the experimental bioreactor

(Figure 3), operated under identical conditions, but having an external sludge recirculation line. The gas permeability of the tubing and the length of tubing used were selected to constantly deliver a specified amount of oxygen by passive diffusion (Table 2).

The performance of both bioreactors was assessed by measuring various parameters: TS and VS destruction was used to evaluating whether microaeration had an impact on solids hydrolysis in the anaerobic digestion process. Biogas production and composition analyses were measured to assess the impact of microaeration on methanogenic activity. The concentration of H_2S in the biogas was measured to evaluate the hypothesis that microaeration reduces H_2S in the biogas. In addition to these parameters, pH and volatile fatty acid concentration in the sludge were monitored. The following sections present the results obtained from these metrics.

Chronological description of overall operational period

Start up and acclimation period. Both bioreactors were seeded with fresh sludge from the full-scale methanogenic bioreactor on May 14, 2023. Both bioreactors were set up without a recirculation line, allowing for a period of acclimation without microaeration. The bioreactors were operated under these conditions for 26 days, which was equal to the SRT of the bioreactors. During this acclimation period, TS and VS concentrations remained statistically similar between the two bioreactors (Figure 5A) and the biogas production rate was slightly higher in the Experimental bioreactor (Figure 5B). The concentration of volatile fatty acids was also similar in both bioreactors (Figure 5C). The main difference between the two bioreactors was the H_2S concentration in the biogas, which increased in the Experimental bioreactor but remained low in the Control bioreactor despite neither bioreactor receiving ferric chloride addition (Figure 3D).

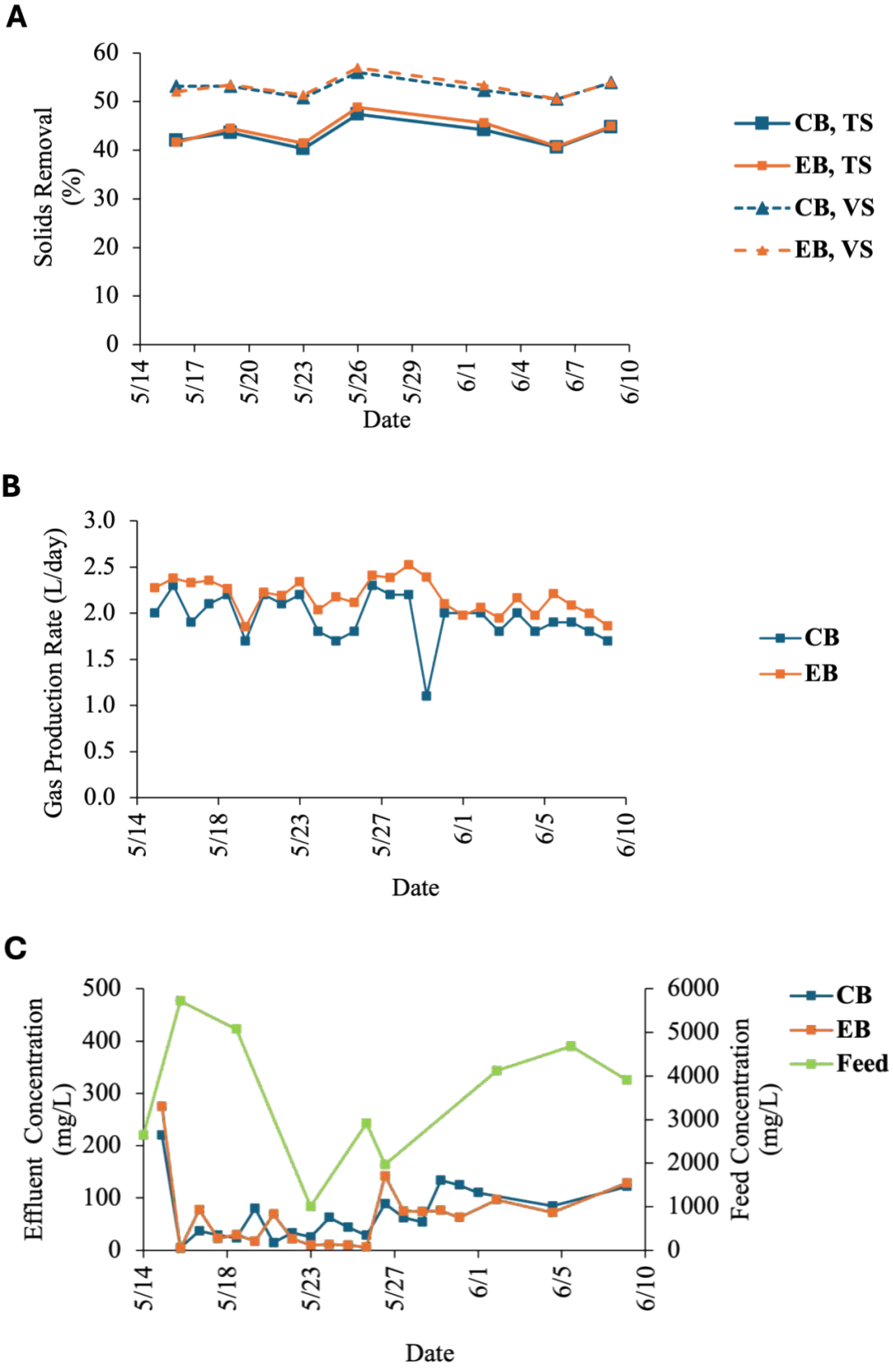
A
Solids Removal (%)
60
50
40
30
20
10
0
5/14
5/17
5/20
5/23
5/26
5/29
6/1
6/4
6/7
6/10
Date
CB, TS
EB, TS
CB, VS
EB, VS
B
Gas Production Rate (L/day)
3.0
2.5
2.0
1.5
1.0
0.5
0.0
5/14
5/18
5/23
5/27
6/1
6/5
6/10
Date
CB
EB
C
Effluent Concentration (mg/L)
500
400
300
200
100
0
Feed Concentration (mg/L)
6000
5000
4000
3000
2000
1000
0
5/14
5/18
5/23
5/27
6/1
6/5
6/10
Date
CB
EB
Feed

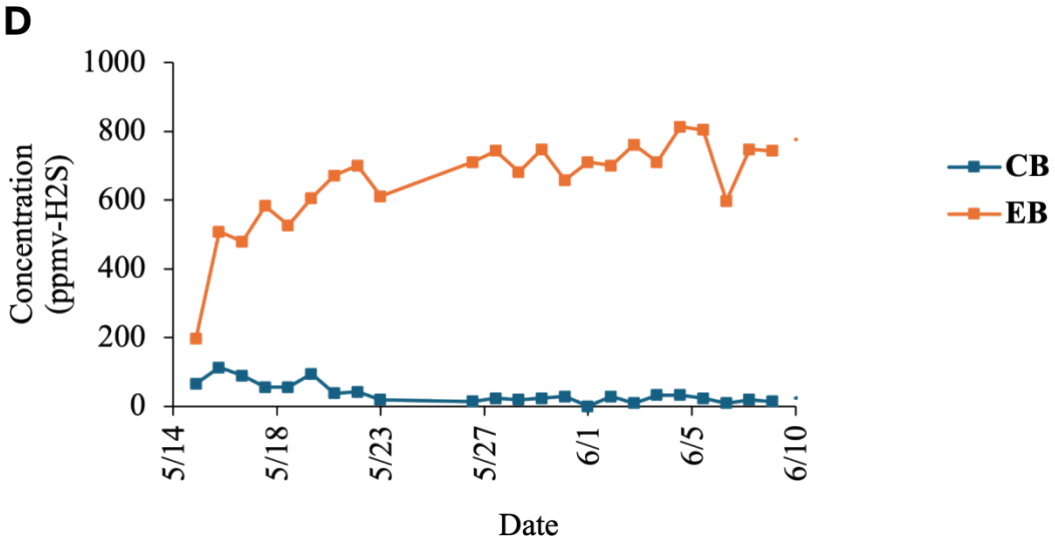

Figure 5. Operation parameters during the start-up and acclimation period. During this period there was no significant difference between the control bioreactor (CB) and the experimental bioreactor (EB) in terms of TS and VS concentration (A), biogas production (B), and VFA concentration (C). However, the H_2S concentration in the biogas from CB remained low while the EB trended per expectation.

Preliminary microaeration periods. Following the acclimation period, the short-term effect of microaeration over solids destruction and H_2S concentration in the biogas of the methanogenic phase anaerobic digester was tested on the Experimental bioreactor. On June 9, 2023, the recirculation line was set up in the Experimental bioreactor (Figure 3). With the initial length and type of tubing used, the oxygen dose in this initial condition was estimated to be at 54.6 $mL_{O2}/L_{reactor}$-day. This preliminary microaeration period (P1) resulted in an immediate reduction in the H_2S concentration in the Experimental bioreactor, from about 740 ppm to about 80 ppm. This operational condition was maintained for 5 days, until June 14, 2023, at which point the recirculation line was disconnected and the bioreactor was continued to be operated without microaeration. At this condition, the H_2S in the biogas of the Experimental bioreactor returned to similar levels as before the introduction of microaeration (Figure 6A). This reduction was accompanied by an increase in the pH from

7.41 to 7.58 after 5 days which came down to 7.41 after 3 days of removal of the recirculation line (Figure 6B). There was no significant change in VFA concentration, solids concentration, or biogas production (Figure 6C, 6D, 6E).

A second preliminary microaeration period (P2) was established on June 22, 2023. In this case, the estimated oxygen dose was 41.2 $mL_{O2}/L_{reactor}$-day. Similar to P1, H_2S concentration dropped, from a 3-day average value of 946 ppm to 256 ppm, and the pH increased from 7.41 to 7.57 upon the addition of oxygen, but no other significant changes were observed (Figure 6). These two preliminary tests confirmed that short-term microaeration led to a reduction in the H_2S in the biogas, and a rise in the pH of the Experimental bioreactor, without any significant changes to VFA concentration, TS and VS concentration, and biogas production. Furthermore, the changes brought about by short-term microaeration to H_2S and pH were reversed once the recirculation line was disconnected from the bioreactor.

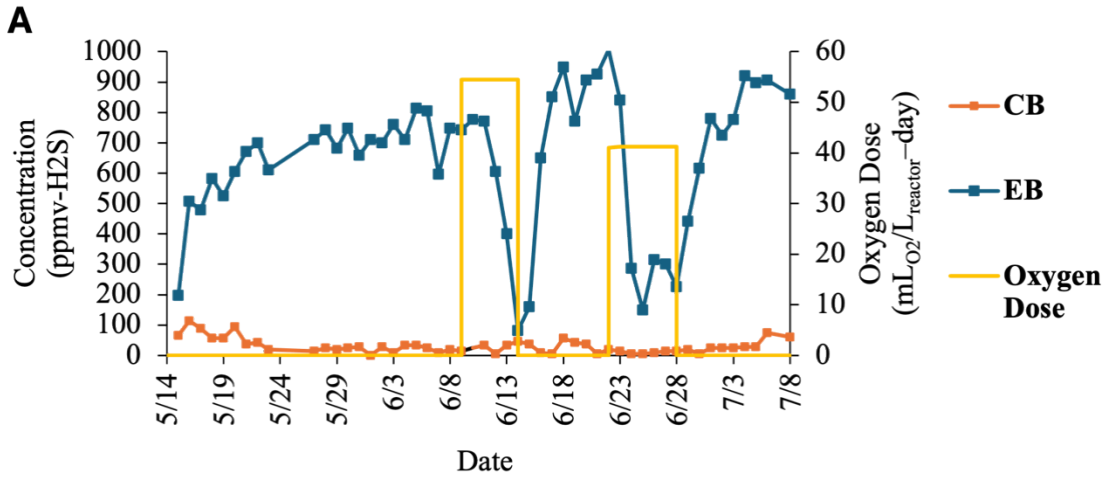

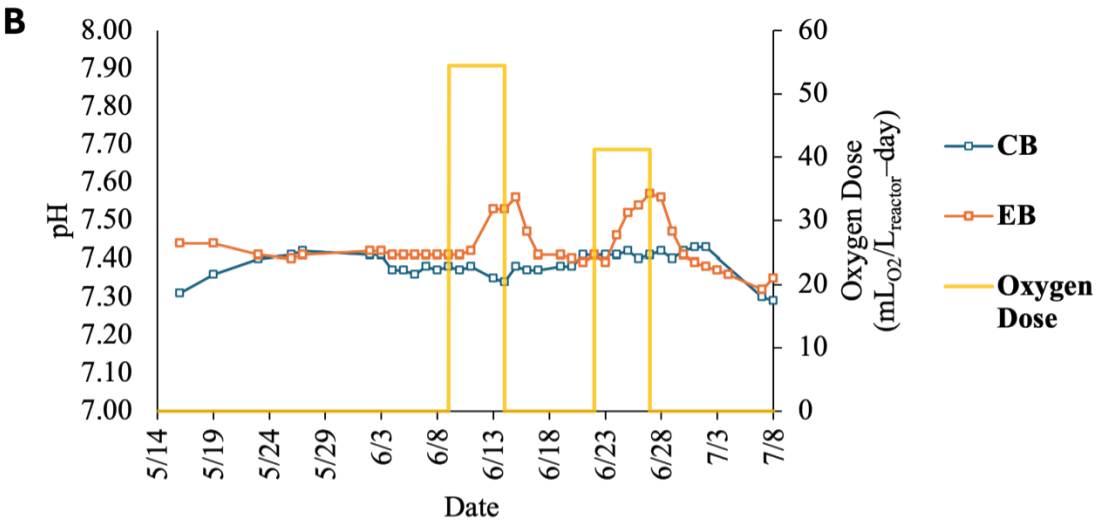
B
pH
Oxygen Dose (mL$_{O2}$/L$_{reactor}$–day)
Date
CB
EB
Oxygen Dose

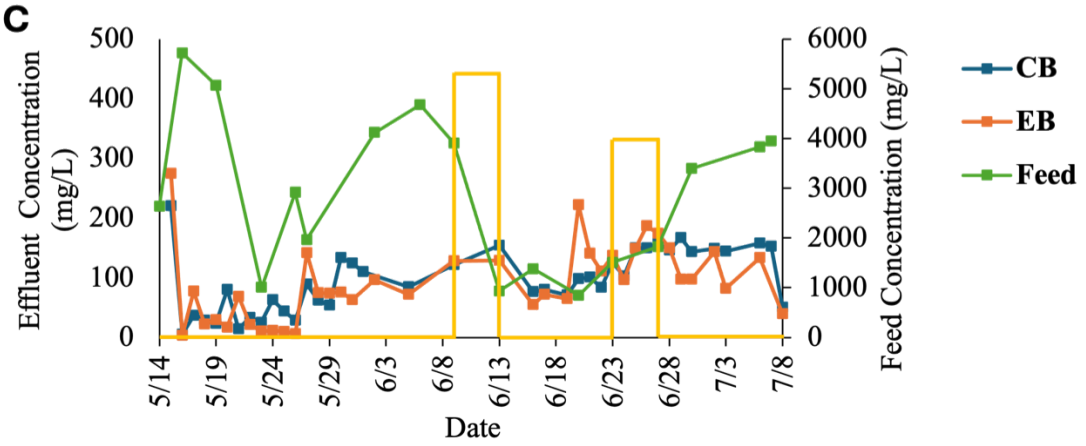
C
Effluent Concentration (mg/L)
Feed Concentration (mg/L)
Date
CB
EB
Feed

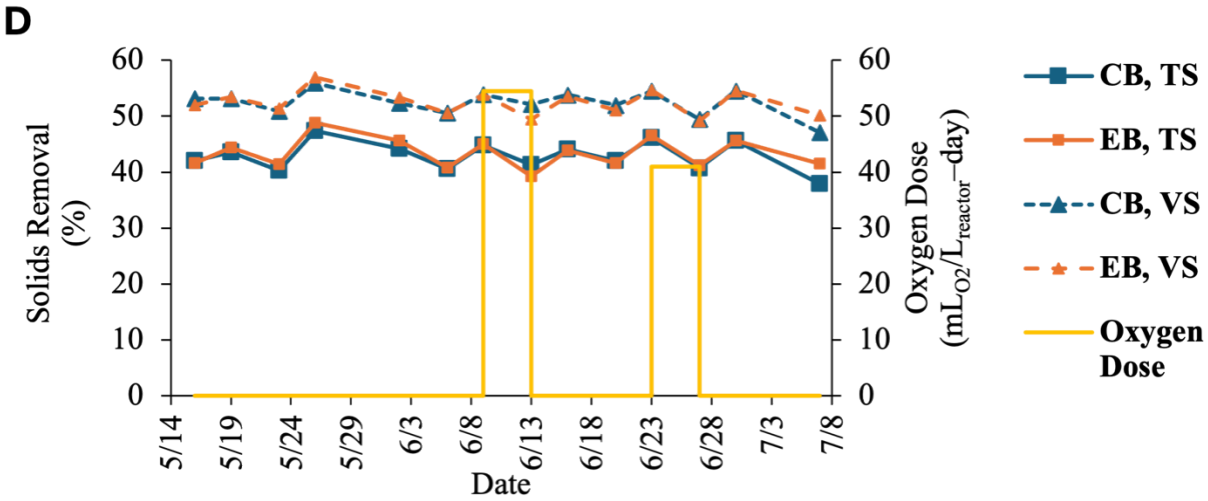
D
Solids Removal (%)
Oxygen Dose (mL$_{O2}$/L$_{reactor}$–day)
Date
CB, TS
EB, TS
CB, VS
EB, VS
Oxygen Dose

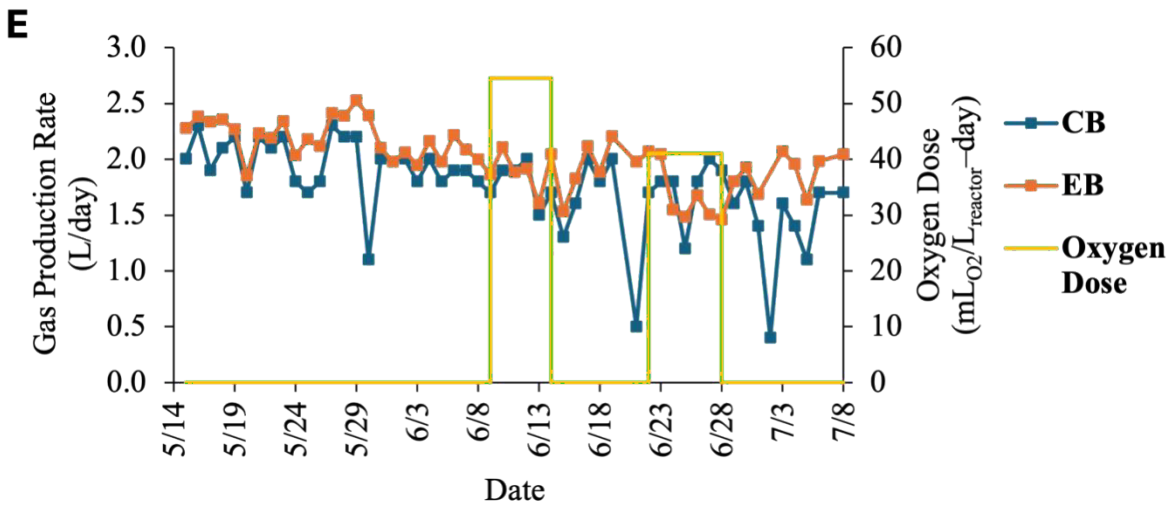

Figure 6. Operation parameters during the start-up period and subsequent preliminary tests, P1 and P2. During this period there was no significant difference between the control bioreactor (CB) and the experimental bioreactor (EB) in terms of TS and VS removal (D), biogas production (E), and VFA concentration (C). However, the H_2S concentration in the biogas (A) showed rapid response to microaeration in EB during the aeration period for both P1 and P2. The rapid increase during the subsequent removal of aeration in EB led to a sharp recovery of H2S in the biogas to even higher than original levels.

Long-term operation under microaerobic conditions. Having established that H_2S concentration in the biogas readily responded to short-term periods of microaerobic conditions, we proceeded to an operational phase with long-term operation (three times the hydraulic retention time) at different oxygen doses. The experimental reactor was operated at four different microaerated conditions, starting at 5.35 $mLO_2/L_{reactor}$-day (D1), followed by a lower dose of 0.67 $mLO_2/L_{reactor}$-day, and then two successively increasing doses of 7.50 and 15 $mLO_2/L_{reactor}$-day (Table 2).

Following the first period at 5.35 $mL_{O2}/L_{reactor}$-day, a leakage through the recirculation line led to uncontrolled amount of aeration of the bioreactor from September 26, 2023, to October 1, 2023. This led to a sharp increase in the pH from 7.17 to 7.71, as well reduced biogas production in the experimental reactor. CH_4 and H_2S concentrations in the biogas also fell to 2.1 %v/v and 28 ppm, respectively (Figure 7). As a result, the recirculation line was

disconnected to prevent further entry of oxygen in the reactor. Furthermore, there was a sharp rise in the total VFA concentration in the effluent of the Experimental bioreactor during the routine operation due to which the influent stream was halted to prevent overloading the reactor with a high organic load in the Experimental bioreactor and to allow the consumption of the accumulated VFAs (Figure 7C). Meanwhile, the effluent extraction was limited to 10mL every 24 hours to monitor the composition of the VFAs.

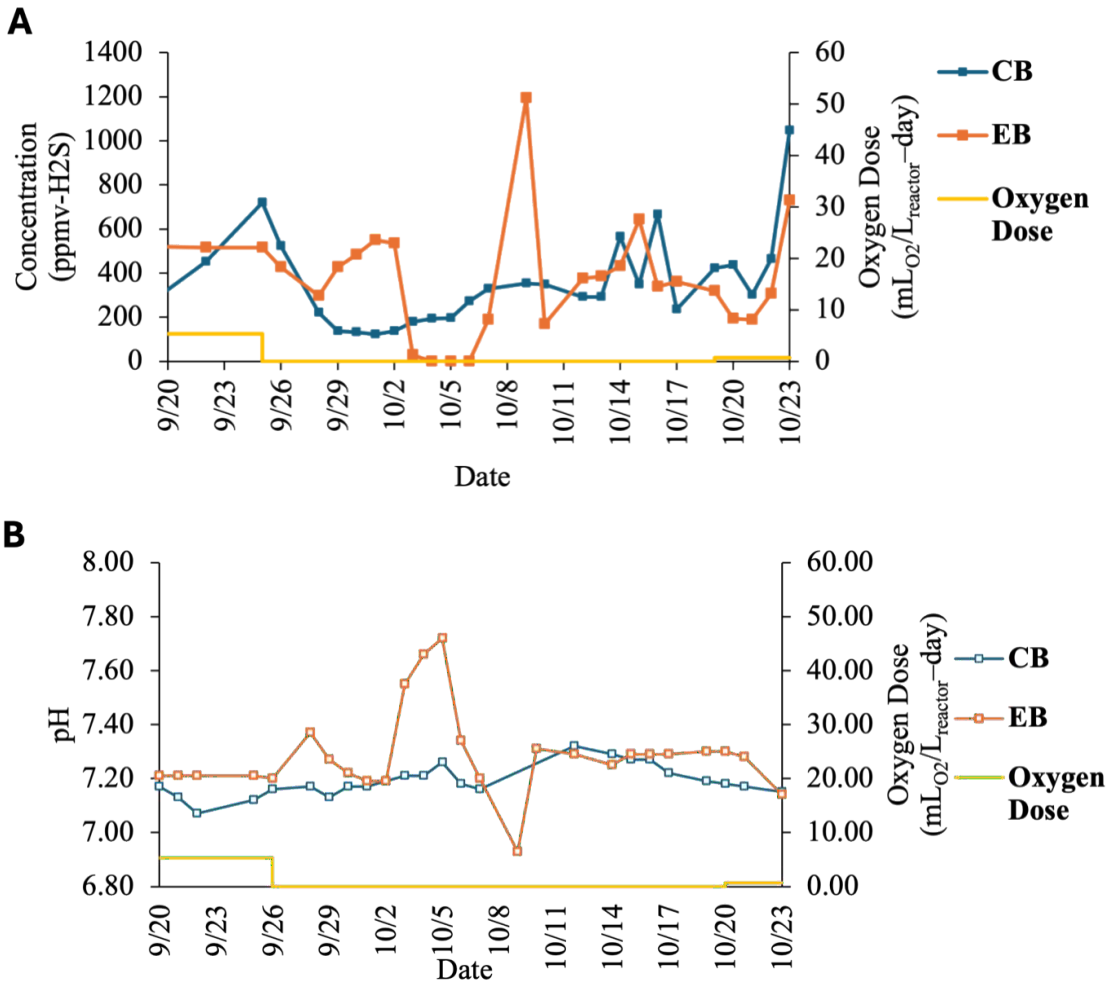

C

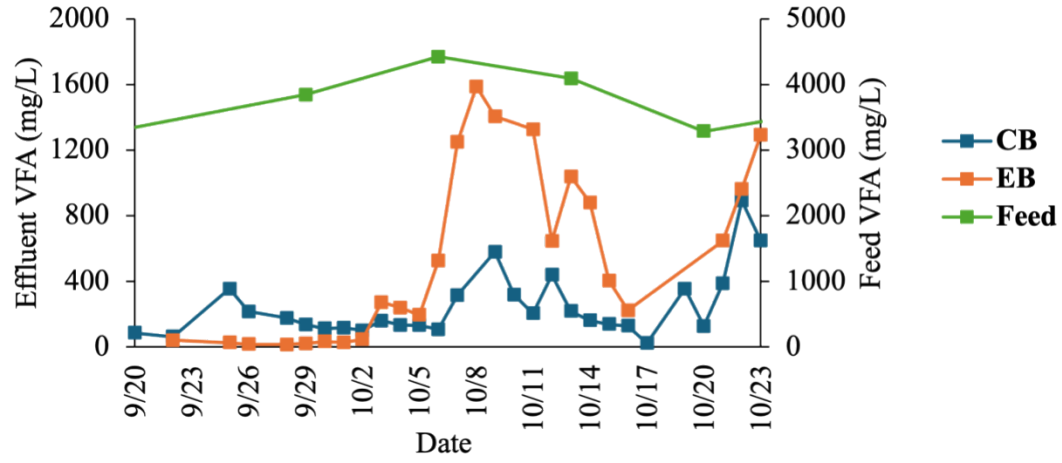
Effluent VFA (mg/L)
Feed VFA (mg/L)
2000
1600
1200
800
400
0
5000
4000
3000
2000
1000
0
9/20
9/23
9/26
9/29
10/2
10/5
10/8
10/11
10/14
10/17
10/20
10/23
Date
CB
EB
Feed

D

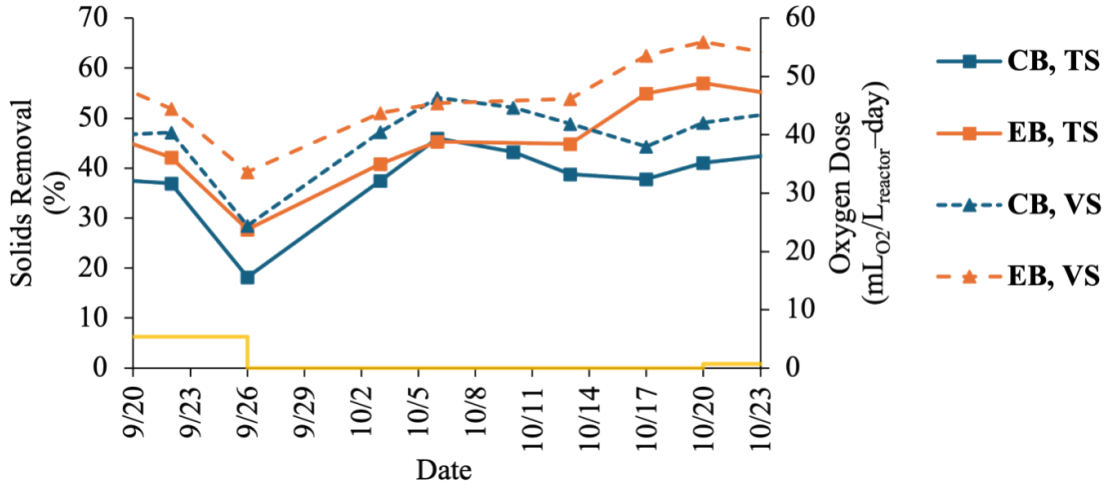
Solids Removal (%)
Oxygen Dose (mL$_{O2}$/L$_{reactor}$–day)
70
60
50
40
30
20
10
0
60
50
40
30
20
10
0
9/20
9/23
9/26
9/29
10/2
10/5
10/8
10/11
10/14
10/17
10/20
10/23
Date
CB, TS
EB, TS
CB, VS
EB, VS

E

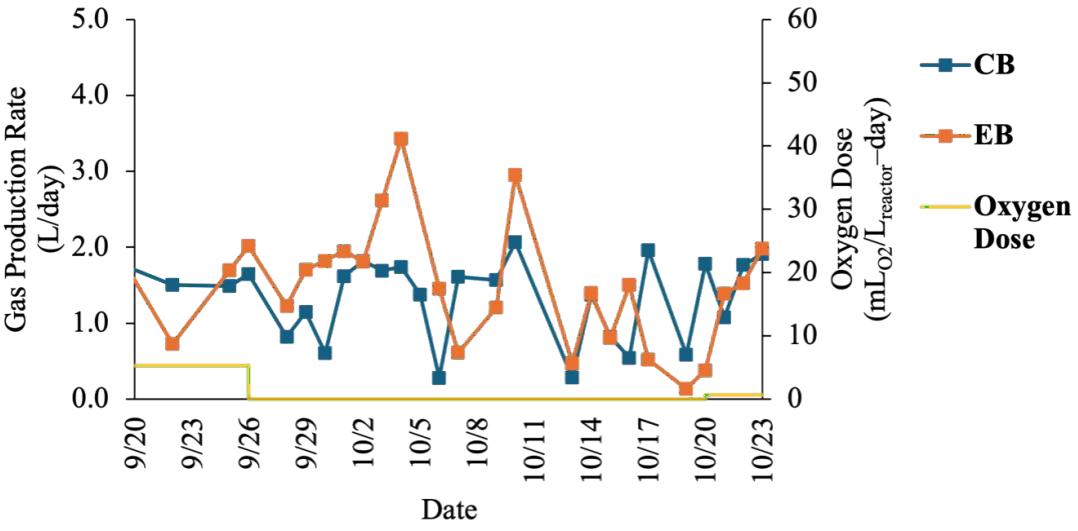
Gas Production Rate (L/day)
Oxygen Dose (mL$_{O2}$/L$_{reactor}$–day)
5.0
4.0
3.0
2.0
1.0
0.0
60
50
40
30
20
10
0
9/20
9/23
9/26
9/29
10/2
10/5
10/8
10/11
10/14
10/17
10/20
10/23
Date
CB
EB
Oxygen Dose

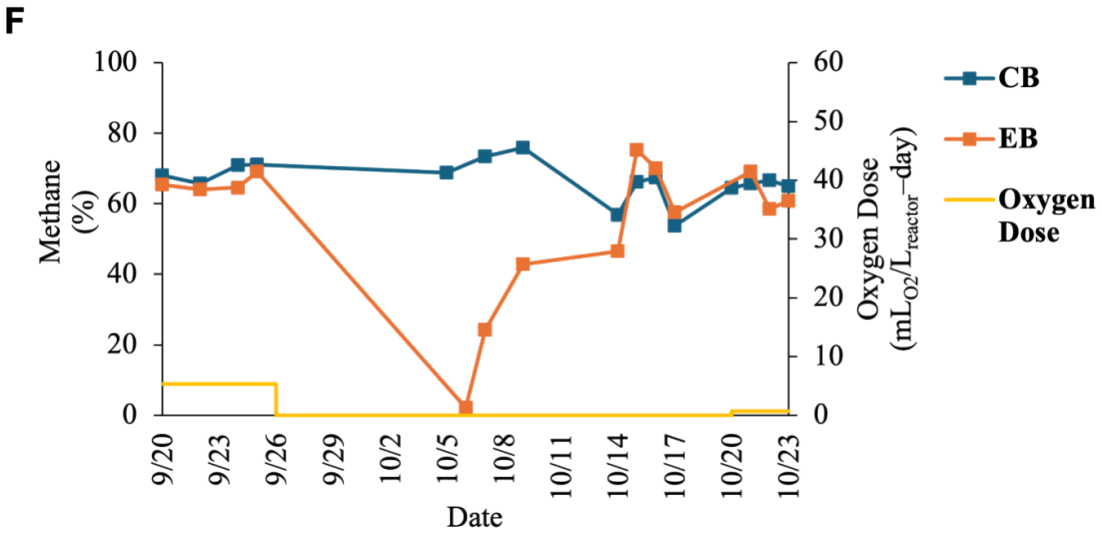

Figure 7. Operation parameters during the period of disruption. There was a sharp rise in the total VFA concentration in the effluent of the Experimental bioreactor during the routine operation due to which the Experimental bioreactor was not fed to allow the consumption of the accumulated VFAs (C). During this period there was significant difference between the control bioreactor (CB) and the experimental bioreactor (EB) in terms of H_2S concentration in the biogas (A), VFA concentration (C), TS and VS removal (D), and the fraction of CH_4 in the biogas (F). The biogas production rate remained comparable in both the bioreactors (E). There was a sharp fall and subsequent recovery of H_2S in the biogas due to the leaking recirculation line and after the removal of leaking recirculation line, respectively, reaching even higher than original levels.

By October 19, 2023, the depleted biogas production had started to recuperate along with higher CH_4 and H_2S concentrations in the biogas produced returning to levels corresponding to the unaerated period of operation. The concentration of VFAs had also gone down from 1588 mg/L on October 8, 2023, to 224 mg/L. Thus, starting October 20, 2023, the routine operation was resumed with a recirculation line corresponding to 0.7 $mL_{O2}/L_{reactor}$-day.

This period informed about the possible indicators to look for while operating anaerobic digesters with microaeration to allow timely intervention in the event of over-aeration of the anaerobic environment. The rapidly increasing pH was the most visible indicator that can be used online, as other indicators require chemical analyses that are not

always available due to lack of high-throughput analytical techniques for measurement. Furthermore, the results from this period were not used for any comparative analyses later in the investigation.

Comparative analysis of solids destruction

According to the literature of microaeration in anaerobic digestion, it had been suggested that microaeration would lead to an increase in VS and TS destruction by enhancing hydrolysis in the AD process (Chen et al., 2020; Fu et al., 2023). This would occur if the activity of facultative hydrolytic fermentative microorganisms is facilitated by the presence of small amounts of oxygen in the sludge (Chen et al., 2020; Fu et al., 2023). Figure 8 presents the measured TS and VS concentrations, respectively, in the feed and in the effluent of the control and experimental reactors. When averaged over the entire period of operation, the average TS concentration in the control and experimental reactors were 2.73 $\pm$ 0.15% w/w and 2.54 $\pm$ 0.14% w/w, respectively (211 samples tested; see Table S1). There was a statistical difference in the two averaged values, at 95% confidence level ($p < 0.001$). Similarly, the averaged VS concentrations in the Control and Experimental bioreactor were 1.91 $\pm$ 0.12% w/w and 1.78 $\pm$ 0.12% w/w (211 samples tested; see Table S1). This difference was also statistically significant at 95% confidence ($p < 0.001$).

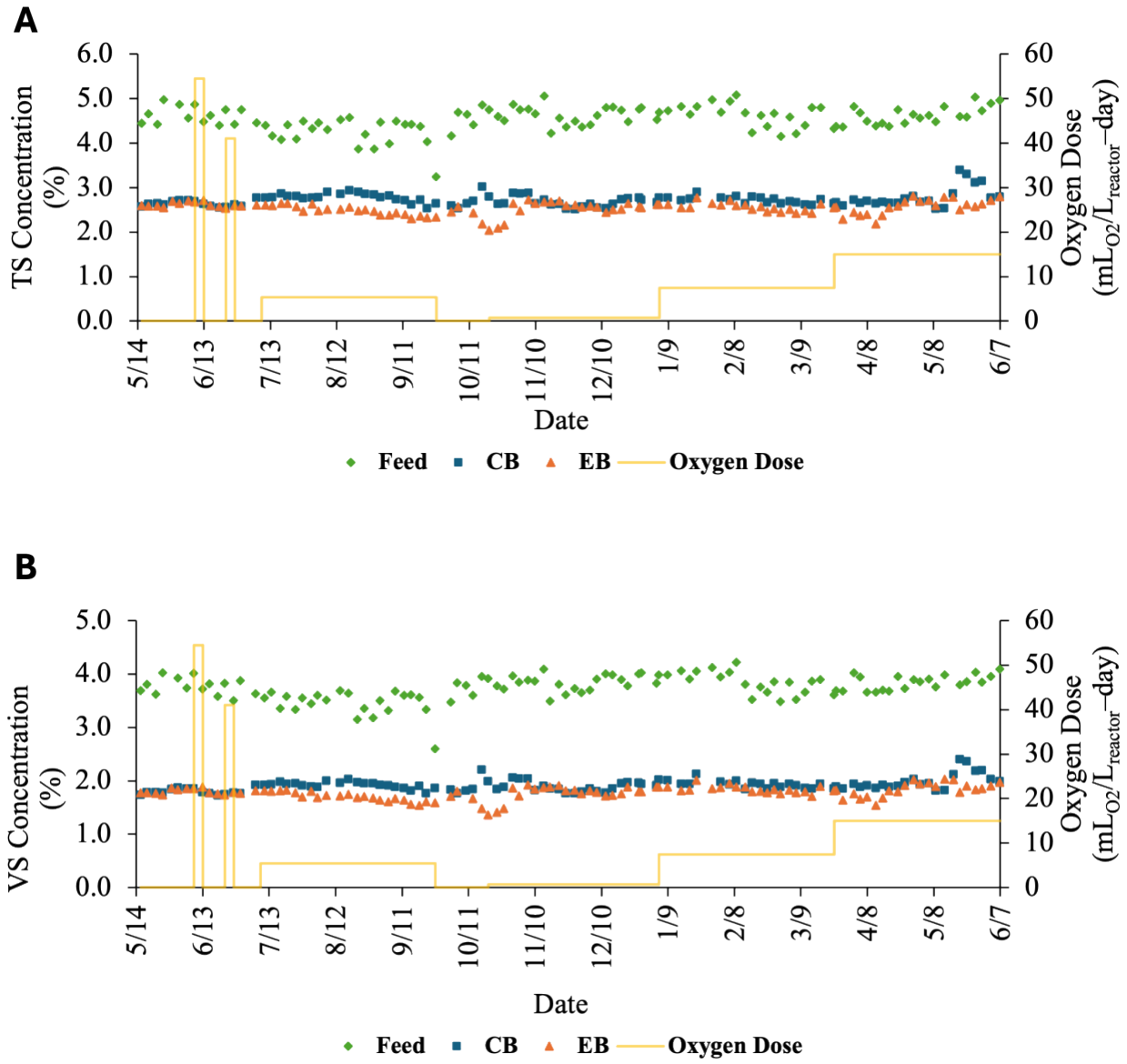

Figure 8. Total solids (A) and volatile solids (B) concentrations in the feed and effluent of the control and experimental reactors throughout the operation of the bioreactors.

The efficiency of TS and VS destruction in the experimental reactor as a function of the different rates of oxygen delivery was also analyzed (Figure 9, Figure 10 and Table S2). Although there were statistical differences in the TS destruction in the experimental reactor for the different periods of oxygen delivery (Figure 10A), a positive trend of increasing TS destruction upon increasing oxygen delivery was not evident. Furthermore, the differences

in observed VS destruction for the different aeration periods were not statistically different at the 95% confidence (Figure 10B).

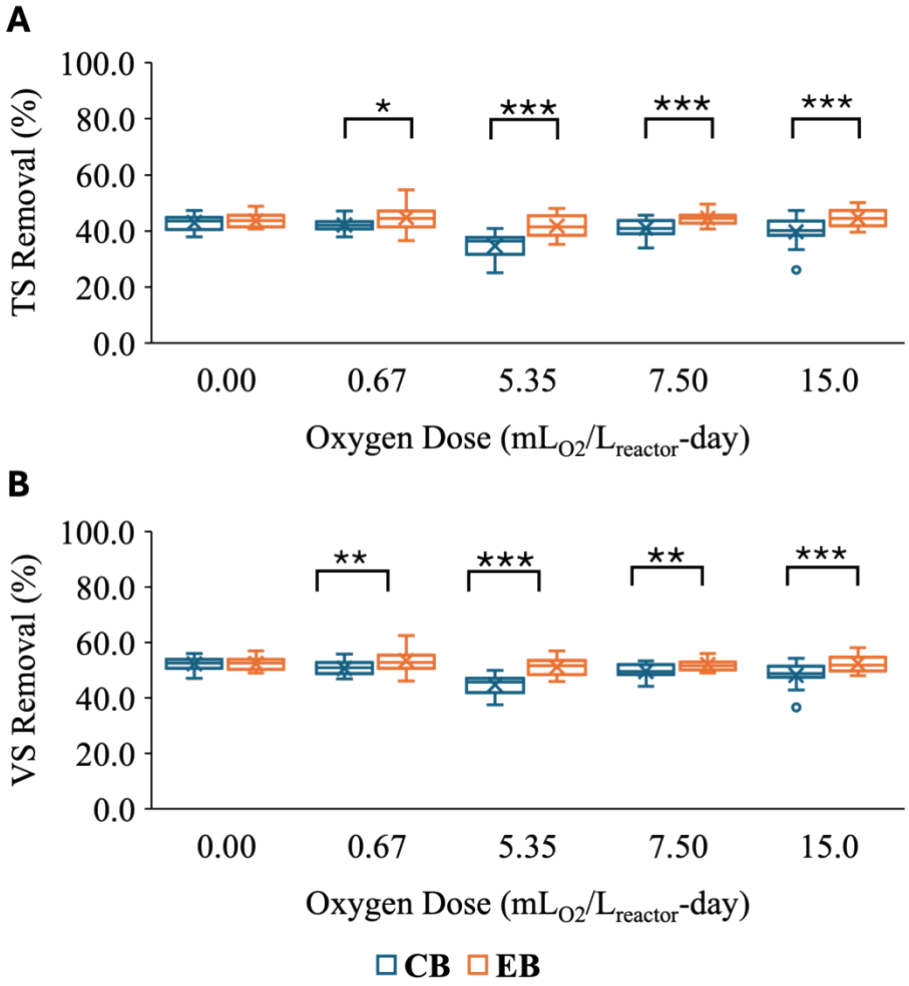

Figure 9. Total solids (A) and volatile solids (B) removal efficiencies as a function of oxygen dose in EB, compared to the removal efficiencies in CB. Unpaired, two-sided Welch's t-tests were performed, and statistically different pairs are indicated for those pairs with statistically significant differences. The rectangular brackets and asterisks indicate p-values less than 0.001 (***), between 0.001 and 0.01 (**), and between 0.01 and 0.05 (*).

It could be concluded from these observations that although there was a statistical difference between the TS and VS concentrations measured in the control and experimental reactors (Figures 9A and 9B), the difference could not be explained by the oxygen addition

to the experimental reactor (Figures 10A and 10B). Based on these observations, the addition of oxygen to the bioreactors, under the conditions of this study, did not alter the rate of solids hydrolysis, and thus, the hypothesis was false.

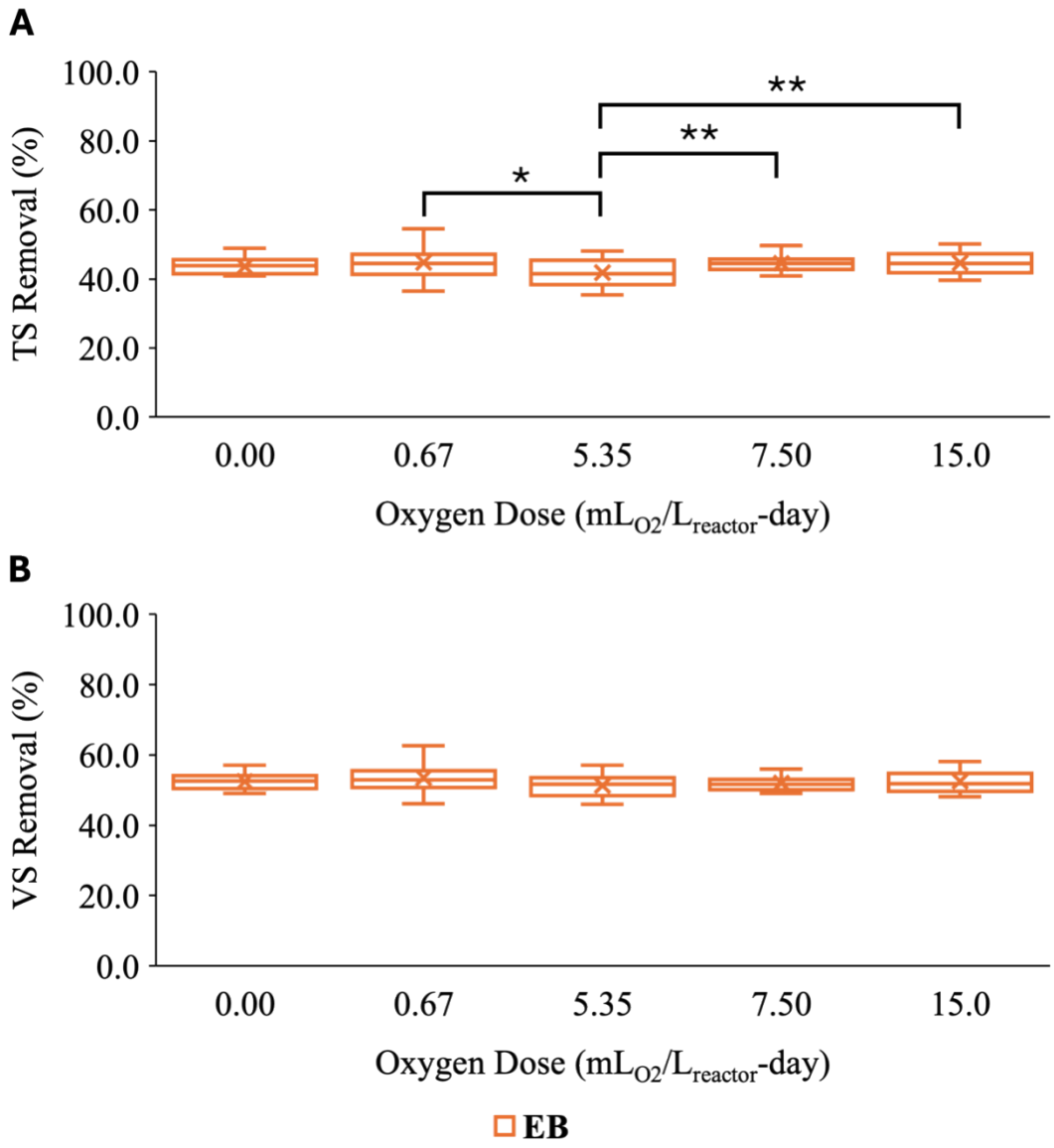

Figure 10. Total solids (A) and volatile solids (B) removal efficiencies as a function of oxygen dose in EB. Unpaired, two-sided Welch's t-tests were performed, and statistically different pairs are indicated for those pairs with statistically significant differences. The rectangular brackets and asterisks indicate p-values less than 0.001 (***), between 0.001 and 0.01 (**), and between 0.01 and 0.05 (*).

Comparative analysis of biogas production

Biogas production in the bioreactors was measured by continuous collection of the produced gas in bags, and then measuring the amount of gas collected by displacing water in an inverted graduated measuring cylinder (Table S3), alongside online measurement using a respirometer (Table S4). Both approaches to measuring gas production showed large variability between subsequent samples in both reactors (Figure 11A, and 11B). The average biogas production rate in the control and experimental reactors for the entire operational period were 1.43 ± 0.30 L/day and 1.85 ± 0.21 L/day, respectively. A comparative analysis of the average gas production rates indicated that there was a statistical difference between these averages, at the 95% confidence (p value < 0.001).

However, there was a noticeable trend of decreasing gas production from the reactor startup on May 14, 2023, until the end of the year, and then an increase from December until the end of operation to June. Since this trend was observed in both reactors (Figure 11A, and 11B), the observation was likely the result of changes in the feed due to seasonal variation.

To evaluate whether any variation in biogas production could be attributed to oxygen input to the experimental reactor, biogas production rates in this reactor as a function of oxygen dose were compared (Figure 12A). There were statistically significant differences when comparing average biogas production rates at the different oxygen doses. There was a drop in the average rate of gas production, from 2.08 ± 0.22 L/day to 1.68 ± 0.45 L/day, as the reactor aeration increased from 0.00 to 0.67 $mL_{O2}/L_{reactor}$-day. The biogas production rate remained similar as the oxygen dose moved from 0.67 $mL_{O2}/L_{reactor}$-day to 5.35 $mL_{O2}/L_{reactor}$-day and increased from 1.65 ± 0.40 L/day to 1.94 ± 0.37 L/day and then to 2.07 ± 0.35 L/day as the dose of oxygen increased from 5.35 $mL_{O2}/L_{reactor}$-day to 7.50 $mL_{O2}/L_{reactor}$-day to 15.0

$mL_{O2}/L_{reactor}$-day, respectively. However, since this variability could relate to seasonal variations in the feed to the bioreactor, an additional analysis was performed where the difference in biogas production between the experimental and control reactors as a function of oxygen dose was evaluated (Figure 12B). This analysis suggested that the variations in the experimental reactor were also observed in the control reactor and thus, supported the hypothesis that the trends in the biogas production were a result of seasonal variations from the feedstock.

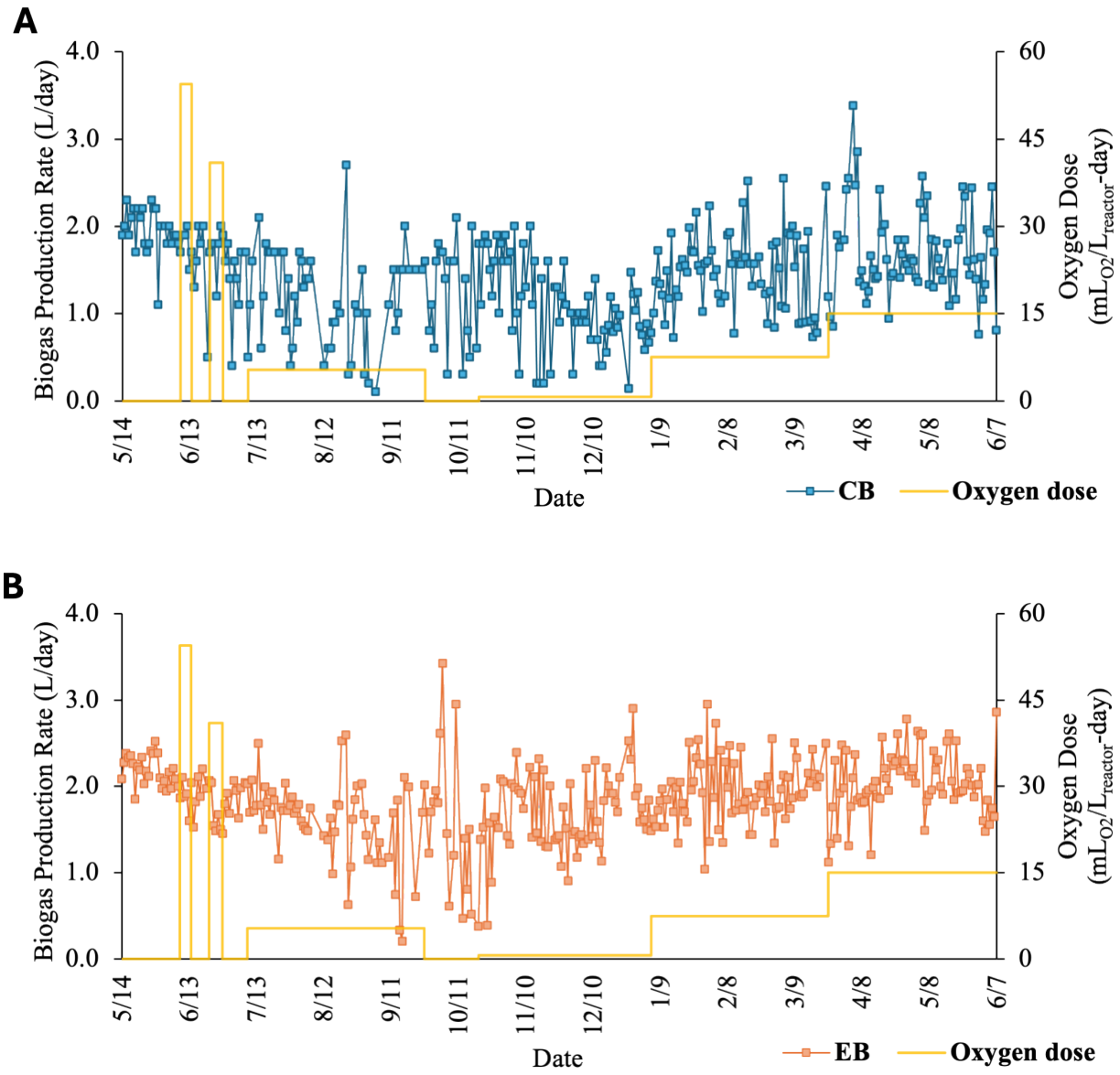

Figure 11. Daily biogas production rate time series for (A) the Control bioreactor and (B) the Experimental bioreactor.

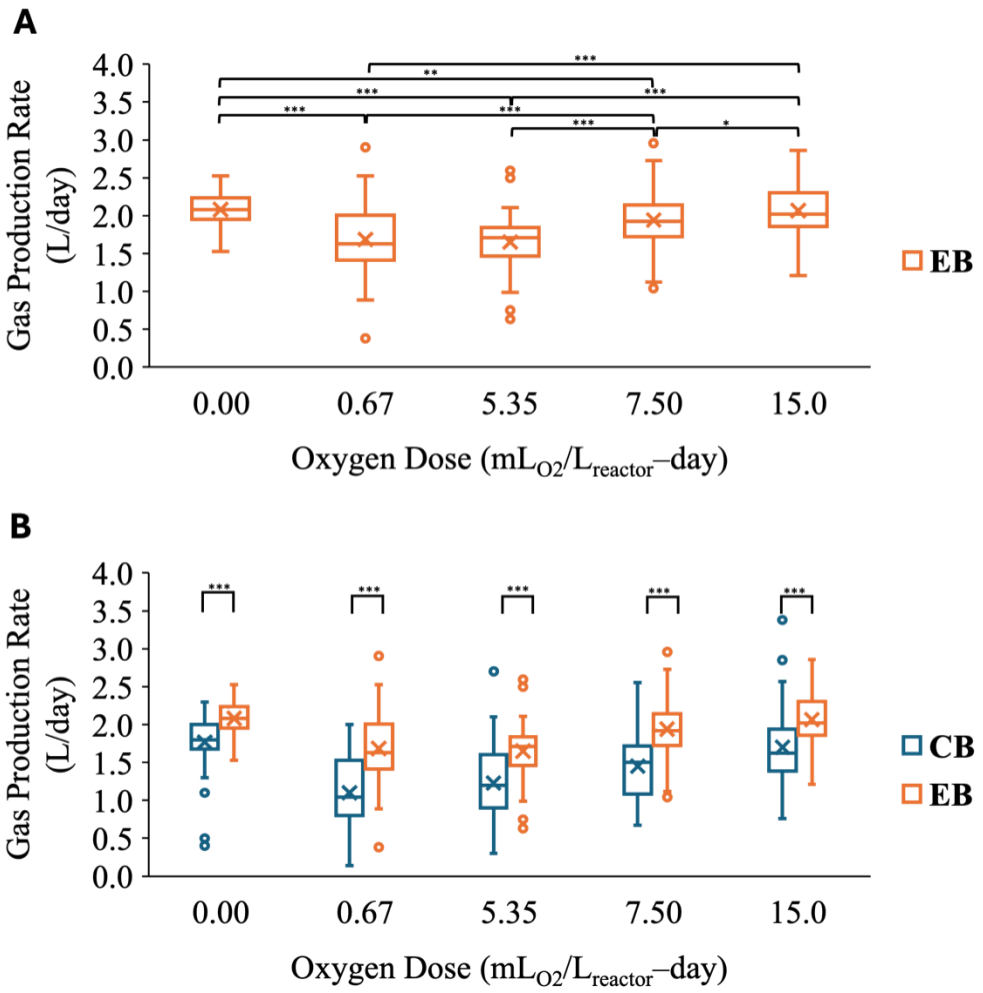

Figure 12. (A) Box plot of daily biogas production rate as a function of oxygen dose in the Experimental reactor. (B) Box plot comparing daily biogas production rates in the Control and Experimental reactors for the operational periods in which the Experimental reactor received different oxygen doses. Unpaired, two-sided Welch's t-tests were performed, and statistically different pairs have been indicated for the pairs with statistically significant differences. The rectangular brackets and asterisks indicate p-values less than 0.001 (***), between 0.001 and 0.01 (**), and between 0.01 and 0.05 (*).

Comparative analysis of biogas composition

The biogas produced by the two bioreactors was collected in gas sampling bags and

subsequently tested daily for the volumetric percentage of CH_4 using a GC–FID from May 15th, 2023, to December 7th, 2023. Following this period, The volumetric percentage of CH_4, CO_2, O_2, and H_2S. The concentration of H_2S in the biogas collected in the gas sampling bags was measured daily by using two portable gas composition analyzers (Tables S8 and S9).

Hydrogen Sulfide: The concentration of H_2S in the biogas collected in the gas sampling bags was measured daily by using two portable gas composition analyzers (Figure 13, Tables S8 and S9).

The concentration of H_2S in the biogas collected showed very high variance across the entire period of operation, as the average values for control and experimental reactors were 480 ± 620 ppm, and 400 ± 210 ppm, respectively. A comparative analysis of the time series of the values from the two bioreactors showed that there was a statistically significant difference at 95% confidence level ($p = 0.034$).

The concentration of H_2S in the biogas collected from the Control bioreactor showed large variations throughout the period of operation. The average daily H_2S concentration was 480 ± 620 ppm. The H_2S remained at 31 ± 24 ppm for the first 8 weeks of operation and increased to 110 ± 80 ppm over the next 10 weeks. For the following 15 weeks, the H_2S levels rose to 530 ± 390 ppm with a highest and lowest weekly average value of 1500 ± 200 ppm and 170 ± 120 ppm. The H_2S for the remainder of the operation was 800 ± 800 ppm with the lowest and highest average weekly values being 240 ± 50 ppm and 3500 ± 300 ppm, respectively. Both bioreactors were routinely checked for leaks therefore the likelihood of external factors, such as atmospheric oxygen influx, influencing the H_2S production or consumption were expected to be eliminated during maintenance.

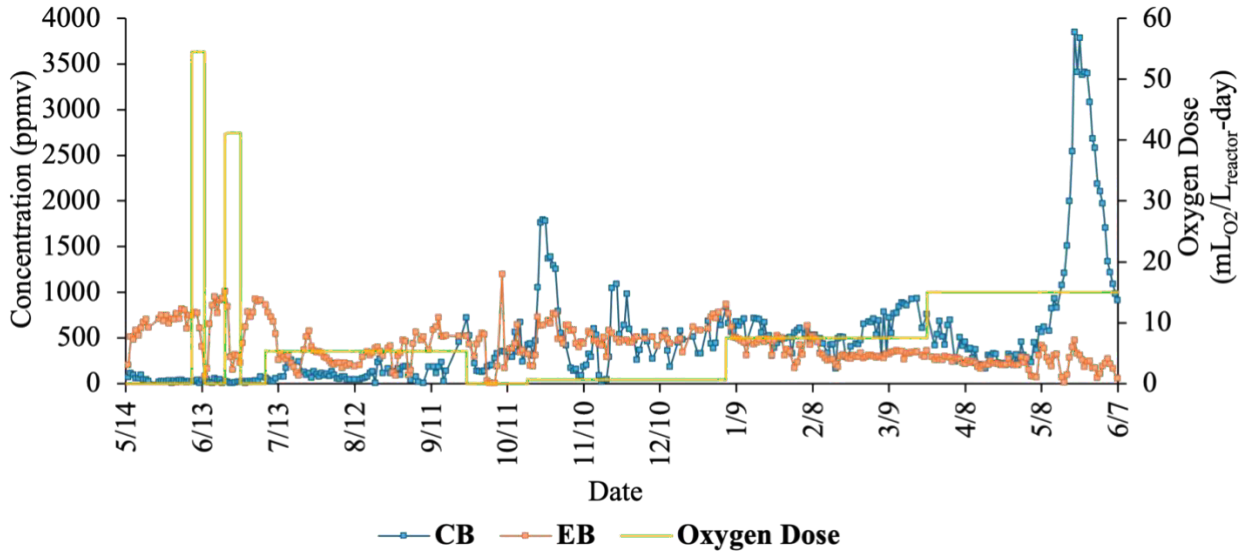

Figure 13. Times series of H_2S concentration in the biogas produced across the entire period of operation of experimental and control bioreactors. The yellow line indicates oxygen dose during the different operational conditions.

Initial tests at high oxygen doses of 54.6 $mL_{O2}/L_{reactor}$–day, and 41.2 $mL_{O2}/L_{reactor}$–day in the control reactor indicated that the response to microaeration was rapid with respect to H_2S concentration in the biogas (Figure 6A). The addition of a recirculation line delivering a dose of 54.6 $mL_{O2}/L_{reactor}$–day led to an immediate drop in the H_2S from a three-day average of 760 ppm to 210 ppm over 4 days. The removal of the recirculation after a four-day period brought the level of H_2S to a three-day average value of 970 ppm. The repetition of this short-term dose trial with 41.2 $mL_{O2}/L_{reactor}$–day led to a drop to 260 ppm and the subsequent rise to 910 ppm.

When comparing the cumulative performance of the experimental bioreactor over long term operation, there was a noticeable trend showing a decline in the mean values with increasing oxygen dose as the mean value of H_2S showed from 750 $\pm$ 120 ppm at 0.0 $mL_{O2}/L_{reactor}$–day while it was 220 $\pm$ 80 ppm at 15.0 $mL_{O2}/L_{reactor}$–day (Figure 14). The concentration of H_2S at 0.67 $mL_{O2}/L_{reactor}$–day was 530 $\pm$ 140 ppm and dropped to 350 $\pm$

160 ppm at 5.35 $mL_{O2}/L_{reactor}$–day. The H_2S did not show any statistically significant change at 95% confidence level with the increase of oxygen dose from 5.35 $mL_{O2}/L_{reactor}$–day to 7.50 $mL_{O2}/L_{reactor}$–day as it changed from 350 ± 160 ppm to 360 ± 100 ppm ($p = 0.35$).

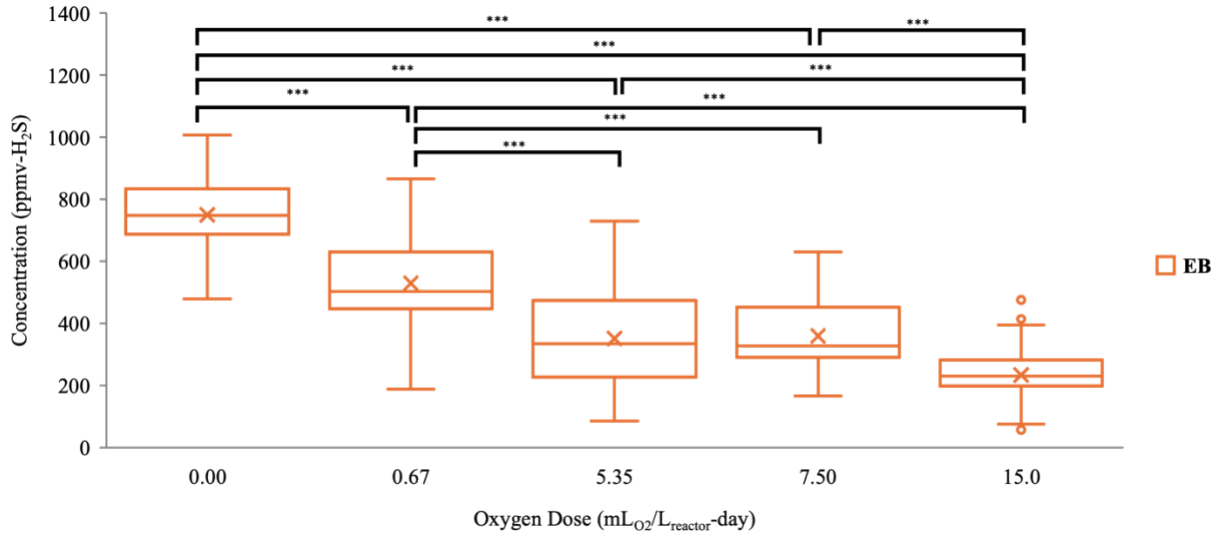

Figure 14. Cumulative H_2S concentration in the experimental and control reactors across the various oxygen doses applied to the control reactor. Unpaired, two-sided Welch's t-tests were performed, and statistically different pairs have been indicated for the pairs with statistically significant differences. The rectangular brackets and asterisks indicate p-values less than 0.001 (***), between 0.001 and 0.01 (**), and between 0.01 and 0.05 (*).

Methane and Carbon Dioxide: A valuable product of the anaerobic digestion process is CH_4–rich biogas, which can be used for energy generation in the form of CHP or, following a purification step, electricity. The volumetric percentage of CH_4 was observed to monitor the health of the digester performance (Figure 15, Table S8).

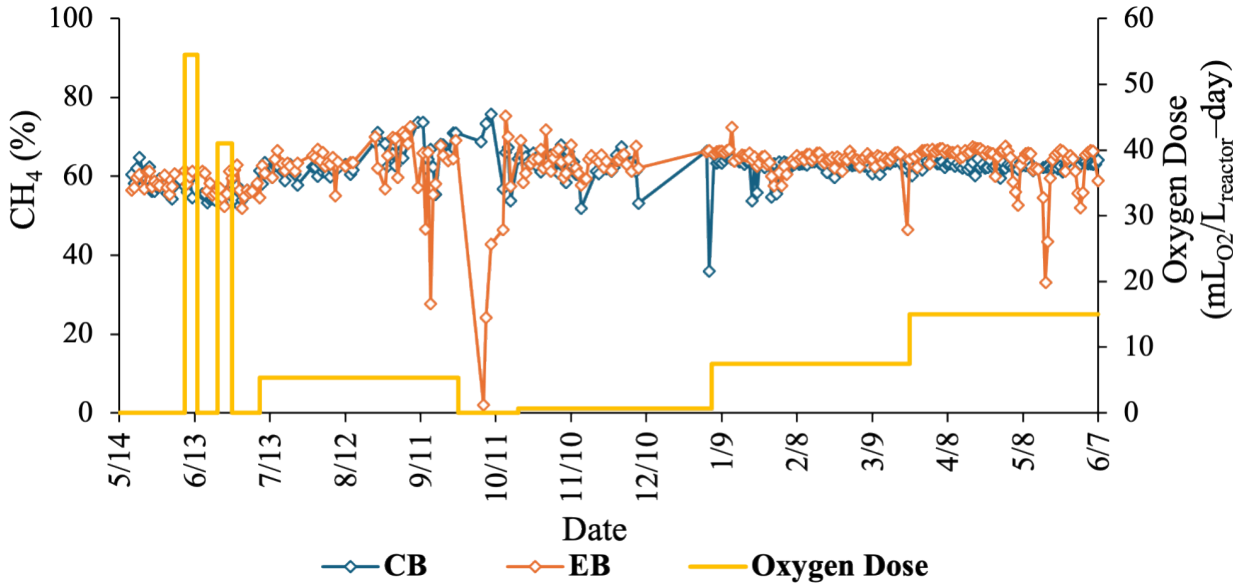

Figure 15. A time series of the fraction of CH_4 in the biogas collected in the sampling bags from the Control and the Experimental bioreactors.

Methanogenic archaea are highly sensitive to oxidative stress and over aeration of the experimental bioreactor showed rapid decrease in the CH_4 fraction in the biogas. This was observed during periods of accidental uncontrolled aeration in the Experimental bioreactor leading to a rapid drop in the CH_4 fraction, from more than 65% to less than 55% of the biogas, once on September 15th, 2023, and on four occasions between March 2024, and the end of the bioreactor operation. Those events did not have any significant impact on the long-term operation under microaeration as the CH_4 returned to former levels within three days of regular operation on each of the instances.

Long-term operation under microaeration showed no negative impact on the fraction of CH_4 in the biogas. There was an increase in the fraction of CH_4 in the biogas collected, in the sampling bags from the Experimental bioreactor, from 58.0 $\pm$ 2.6% during the start-up and acclimation period to 63.7 $\pm$ 4.8% during the period the Experimental reactor was microaerated. An increase was observed in the Control bioreactor, as well, as the fraction of

CH_4 increased from 56.9 $\pm$ 2.7% to 62.9 $\pm$ 2.7% for the corresponding periods. The increase in the Experimental bioreactor was not consistent across the different microaeration doses as there was no statistically significant difference between the fractions of CH_4 of any two of the first three microaeration doses, i.e., 0.67, 5.35, and 7.50 $mL_{O2}/L_{reactor}$—day, which were at 63.6 $\pm$ 3.0% (n = 40), 64.3 $\pm$ 3.9% (n = 47), and 64.4 $\pm$ 2.0% (n = 74), respectively (Figure 16A). However, for the highest microaeration dose, i.e., 15.0 $mL_{O2}/L_{reactor}$—day, the fraction of CH_4 was 65.7 $\pm$ 1.6% (n = 56), which higher than all other microaeration doses, the increase being statistically significant ($p < 0.001$ when compared with 0.67 or 7.50, and $p = 0.011$ when compared with 5.35 $mL_{O2}/L_{reactor}$—day).

The fraction of CH_4 in the biogas from the Control bioreactor was relatively more stable as visible in both Figure 11 and from the lower standard deviation. The average fraction of CH_4 in the Experimental bioreactor when under the different microaeration doses was 63.7 $\pm$ 4.8% (n = 237) which was higher than the 62.7 $\pm$ 2.7% (n = 219) from the Control bioreactor. This difference was statistically significant at 95% confidence level ($p = 0.032$). Furthermore, the fraction of CH_4 in the biogas from the Experimental bioreactor was, on an average, higher that in the Control bioreactor for each of the microaeration doses, as well (Figure 14B).

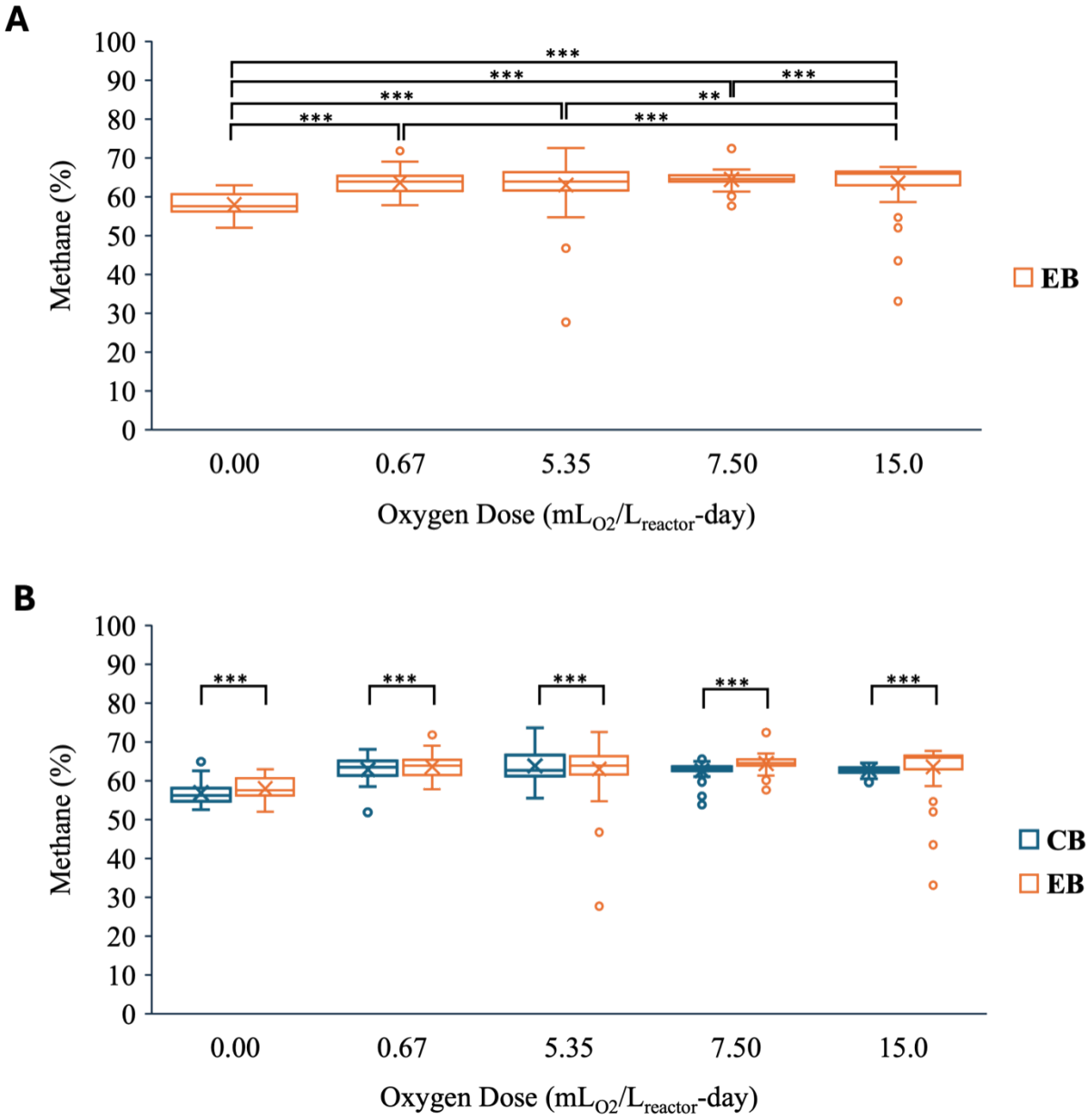

Figure 16. (A) A box plot comparing the fraction of CH_4 in the biogas collected from the Experimental bioreactor across different doses; (B) a box plot comparing the fraction of CH_4 between the Control and Experimental bioreactor across the different microaeration doses in the latter reactor. Unpaired, two-sided Welch's t-tests were performed, and statistically different pairs have been indicated for the pairs with statistically significant differences. The rectangular brackets and asterisks indicate p-values less than 0.001 (***), between 0.001 and 0.01 (**), and between 0.01 and 0.05 (*).

Using the volumetric fractions of CH_4 and CO_2 measured, the ratio of CH_4 to CO_2 was

estimated and it was observed that the ratio was the same for the control bioreactor, at 1.82 $\pm$ 0.1 (n = 138), throughout the period of observation. The ratio was higher in the Experimental bioreactor as it was 2.01 $\pm$ 0.02 (n = 74) at 7.50 $mL_{O2}/L_{reactor}$—day ($p < 0.001$) and 2.20 $\pm$ 0.00 (n = 58) at 15.0 $mL_{O2}/L_{reactor}$—day ($p < 0.001$) (Figure 17B). The increase in the ratio from the Experimental bioreactor was statistically significant ($p < 0.001$).

The CO_2 fraction of the biogas collected in the gas sampling bags was measured for the period when the Experimental bioreactor was under 7.50 and 15.0 $mL_{O2}/L_{reactor}$—day, using a handheld measuring device (Figure 17A and Table S8). The CO_2 fraction in the biogas from the Experimental bioreactor was lower than that in the Control bioreactor, for both sets of the microaeration doses; for 7.50 $mL_{O2}/L_{reactor}$—day, the CO_2 fraction was 32.1 $\pm$ 1.3% (n = 74) in the Experimental bioreactor compared to 34.3 $\pm$ 1.3% (n = 68) in the Control bioreactor, and 29.7 $\pm$ 0.9% (n = 58) against 34.6 $\pm$ 0.8% (n = 70) in the Experimental and the Control bioreactor, respectively, for 15.0 $mL_{O2}/L_{reactor}$—day. The reduction in the CO_2 in the Experimental bioreactor when under 15.0 $mL_{O2}/L_{reactor}$—day compared to 7.50 $mL_{O2}/L_{reactor}$—day was also statistically significant ($p < 0.001$).

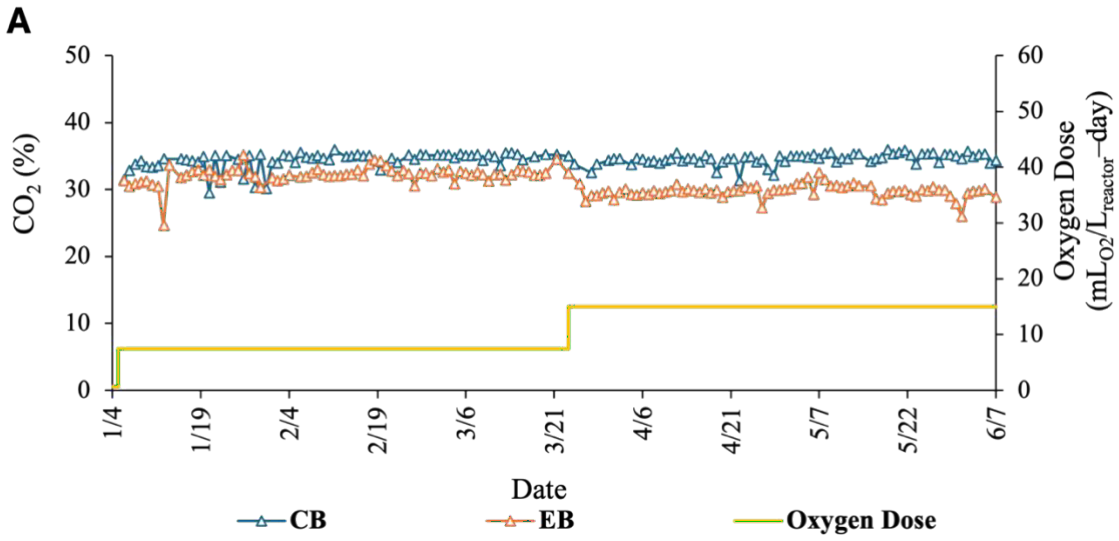

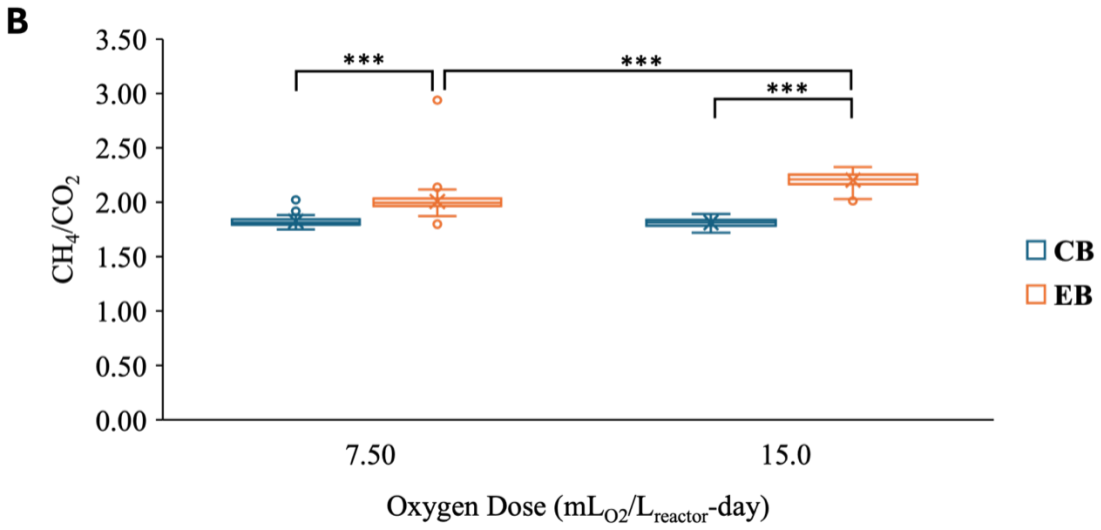

Figure 17. (A) A time series of the fraction of CO_2 in the biogas collected from the Control and the Experimental bioreactors for the microaeration doses of 7.50 and 15.0 $mL_{O2}/L_{reactor}$—day. (B) Box plot comparing the fractions of CO_2 measured during the same period; unpaired, two-sided Welch's t-tests were performed, and statistically different pairs have been indicated for the pairs with statistically significant differences. The rectangular brackets and asterisks indicate p-values less than 0.001 (***), between 0.001 and 0.01 (**), and between 0.01 and 0.05 (*).

Oxygen: The presence of O_2 gas in the biogas could be used to understand if a microaeration dose was low enough to ensure the consumption of the oxygen being supplied into the digester and avoid over–aeration. Thus, the biogas collected in the gas sampling bags was used to measure the presence of O_2 gas in the headspace of both the bioreactors. The O_2 fraction of the biogas collected in the gas sampling bags from both the bioreactors was measured for the period when the Experimental bioreactor was under 7.50 and 15.0 $mL_{O2}/L_{reactor}$—day, using a handheld measuring device (Figure 18 and Table S8).

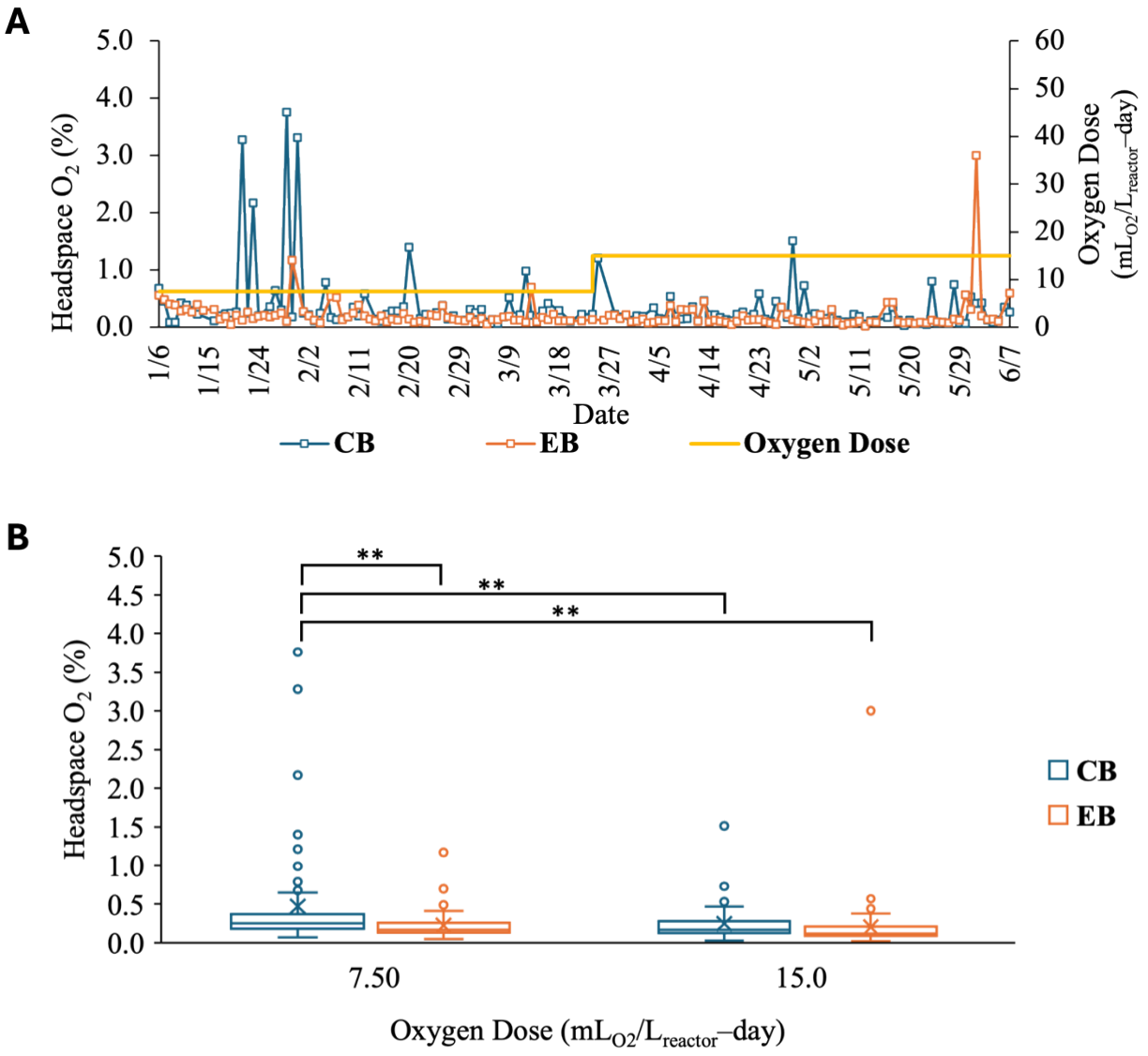

Figure 18. (A) A time series of the fraction of O_2 in the biogas collected from the Control and the Experimental bioreactors for the microaeration doses of 7.50 and 15.0 $mL_{O2}/L_{reactor}$—day. (B) Box plot comparing the fractions of O_2 measured during the same period; unpaired, two-sided Welch's t-tests were performed, and statistically different pairs have been indicated for the pairs with statistically significant differences. The rectangular brackets and asterisks indicate p-values less than 0.001 (***), between 0.001 and 0.01 (**), and between 0.01 and 0.05 (*).

The measurement of O_2 in the biogas collected showed no change ($p > 0.05$) in between the two periods when the microaeration dose in the Experimental bioreactor was increased from 7.50 to 15.0 $mL_{O2}/L_{reactor}$–day as O_2 values were $0.24 \pm 0.17\%$ ($n = 74$) and

$0.20 \pm 0.36\%$ ($n = 72$), respectively.

However, O_2 in the Control bioreactor varied between the two periods as it was $0.47 \pm 0.72\%$ ($n = 69$) and $0.25 \pm 0.23\%$ ($n = 69$) ($p < 0.01$) when the microaeration dose in the Experimental bioreactor was 7.50 and 15.0 $mL_{O2}/L_{reactor}$–day, respectively. There were spikes in the O_2 levels in the biogas collected from the Control bioreactor during the early period when the O_2 measurements were recording the handheld device. While there is no confirmation on what might have had led to those increases, it was suspected to be a result of faults in the sampling bags. Those spikes were also the result of these differences in the measured values.

Comparative analysis of methane yield

Alongside measuring the concentration or quantity of CH_4 in the biogas, it is important to measure the yield of CH_4, Y_{CH4}, in the anaerobic digestion process to understand the impact of microaeration. Yield is a measure of the quantity of CH_4 produced per gram of VS destroyed in the bioreactor. A steady value of Y_{CH4}, following microaeration, would imply that the microbial community was resilient against the change in oxygen stress. An increase in value of Y_{CH4} would suggest that the oxygen stress introduced was catalyzing the overall process of digestion while a decline in the value of Y_{CH4} could suggest that microaeration was exerting a stress on methanogenic activity which was central to the digestion process.

The concentration of CH_4 in the biogas was measured using the gas collected in the sampling bags connected to the bioreactors, first, using a GC-FID, and later using a handheld gas composition analyzer. The rate of biogas production rate was measured using two methods, as well; first, a water displacement method was employed to measure the total amount of biogas collected over a 24-hour period on average, and later online gas production

volume measurement was performed using a respirometer and the volume of biogas produced over 24-hour periods were used for rate calculation. These two quantities were used for measuring the quantity of CH_4 produced by both the bioreactors. Finally, using the VS concentrations in the influent and the effluents, obtained from the tests run at the lab at MMSD, and the influent and effluent flow rates of the bioreactor, the values of Y_{CH4} were estimated using Equations (2) to (7), for both the control and the experimental reactors for the different period of operation (Figure 19, Tables S5 - S7).

The average values of Y_{CH4} across the entire period of operation were 0.67 ± 0.04 L_{CH4}/g_{VS} $(n = 69)$ and 0.75 ± 0.03 L_{CH4}/g_{VS} $(n = 80)$ for the Control and the Experimental bioreactors, respectively. Comparing these two sets of values indicated that microaeration had an overall increase in the value of Y_{CH4} $(p = 0.008)$. Furthermore, the values of the Y_{CH4} in the Control and the Experimental Bioreactors were compared across periods of varying microaeration doses to account for the differences arising due to changes in the feedstock (Figure 16A). This comparison showed that the methane yield was significantly different $(p = 0.034)$ between the two bioreactors only when the Experimental bioreactor was under 7.50 $mL_{O2}/L_{reactor}$—day, with a value of 0.73 ± 0.02 $(n = 19)$ against the value of the Control bioreactor of 0.59 ± 0.04 $(n = 15)$. However, for all other microaeration doses, the value of Y_{CH4} was similar across long term operation for the two bioreactors.

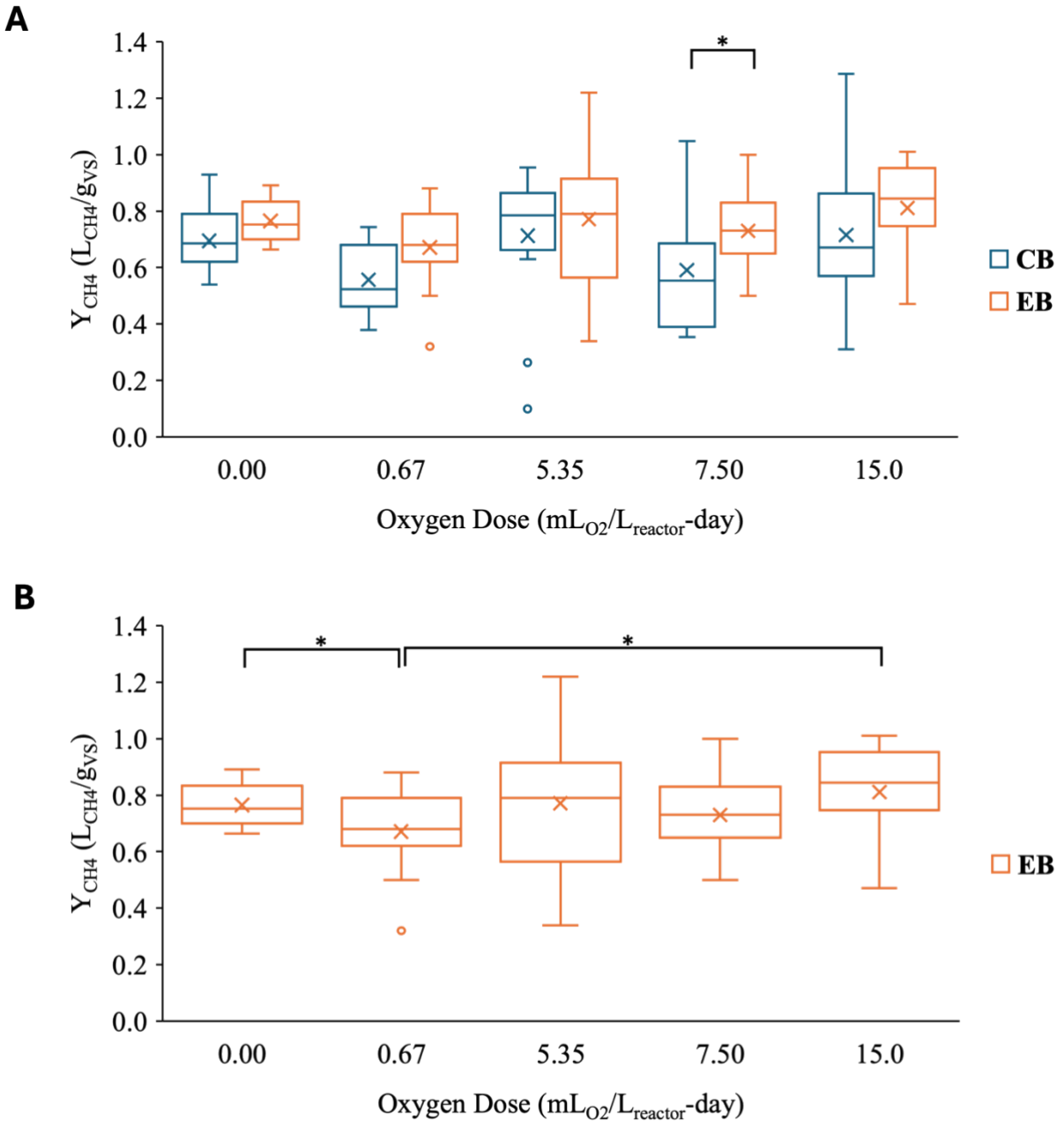

Figure 19. (A) Box plot of methane yield in the Control (CB) and the Experimental (EB) bioreactor to compare the performance of the two bioreactors across the varying microaeration doses in EB. (B) Box plot of methane yield in EB only to compare the performance across the varying microaeration doses. Unpaired, two-sided Welch's t-tests were performed, and statistically different pairs have been indicated for the pairs with statistically significant differences. The rectangular brackets and asterisks indicate p-values less than 0.001 (***), between 0.001 and 0.01 (**), and between 0.01 and 0.05 (*).

When comparing the values of Y_{CH4} from the Experimental bioreactor, there is a drop

during the period when the microaeration dose was 0.67 $mL_{O2}/L_{reactor}$—day as it was 0.67 ± 0.02 L_{CH4}/g_{VS} ($n = 15$) compared to 0.77 ± 0.01 L_{CH4}/g_{VS} ($n = 10$) during the start-up period of the Experimental bioreactor ($p = 0.048$), and 0.81 ± 0.03 ($n = 18$) when the microaeration dose was 15.0 $mL_{O2}/L_{reactor}$—day ($p = 0.015$). However, these changes were observed in the Control bioreactor for the respective periods as well. Thus, these results indicate that microaeration did not have any significant effect on the methane yield from the destruction of volatile solids.

DISCUSSION

Microaeration does not affect solids removal

Hydrolysis, performed by extracellular hydrolytic enzymes, secreted by mainly aerobic or facultative and some anaerobic bacteria, is usually considered the rate-limiting step of AD. Enhancing hydrolysis improves the dissolution of complex organic matter into simpler substrates for subsequent degradation. Thus, hydrolysis is the key step in solids removal and sludge volume reduction (Chen et al., 2020; Fu et al., 2023). It was hypothesized that microaeration would enable the activity of facultative hydrolytic organisms to shift to aerobic respiration and improve solids removal.

The results obtained in this investigation suggest that microaeration, up to 15.0 $mL_{O2}/L_{reactor}$—day, of the methanogenic phase digester in a two stage AD process does not affect solids removal. While there was a significant difference between the solids destruction efficiency between the Control and the Experimental bioreactor throughout the period of operation under when the Experimental bioreactor was under microaeration, the steady level of removal efficiency and lack of noticeable trends with increasing microaeration doses would suggest that these changes may not have been due to microaeration.

CH_4 fraction of the biogas increased with microaeration at higher concentration

There was increase in the CH_4 fraction in the biogas from, both, the Control as well as the Experimental bioreactor. This increase might have been due to changes in operation conditions such improved mixing in a bench scale reactor compared to a full-scale anaerobic digester. The lack of any significant increase in CH_4 until 7.50 $mL_{O2}/L_{reactor}$—day (Figure 14) suggested that the microaeration did not affect biogas production. A statistically significant change was observed only after increasing the microaeration dose to 15.0 $mL_{O2}/L_{reactor}$—day.

This suggested that microaeration could assist in increasing the CH_4 fraction at relatively higher doses. The lack of changes in Y_{CH4} (Figure 18) suggested that the increase in CH_4 was not likely a result of hydrolysis but rather during the later stage of the AD process.

Methane production is achieved by a combination of two major pathways in the AD process — acetoclastic methanogenesis, i.e., conversion of acetic acid to CH_4 and CO_2, and hydrogenotrophic methanogenesis, i.e., conversion of H_2 and CO_2 to CH_4 and H_2O (Figure 1). Under most conditions, methanogenesis is dominated by acetoclastic methanogenesis (~75%) (Khanal, 2008). It had been observed that microaeration favored a shift to the dominance of hydrogenotrophic methanogenic archaea, such as the genera *Methanosarcina* and *Methanobrevibacter*, in methane production. This may have likely been due to the presence of oxygen detoxifying enzymes, such as superoxide dismutase, catalase and peroxidase, which might be responsible for oxygen tolerance in micro-aeration conditions (Fu et al., 2023; Nguyen et al., 2019).

As hydrogenotrophic methanogenesis involves CO_2 reduction for CH_4 production, it may also reduce the CO_2 fraction of the biogas. A decrease in the CO_2 fraction was observed in the Experimental bioreactor as the microaeration dose increased from 7.50 to 15.0 $mL_{O2}/L_{reactor}$–day from $32.1 \pm 1.3\%$ to $29.7 \pm 0.9\%$, respectively, while no significant changes were observed in the Control bioreactor (Figure 17A). Furthermore, on comparing the ratio of the volumetric fractions of CH_4 to CO_2 in the biogas (Figure 17B), there was a significant increase in the ratio from 1.83 ± 0.00 to 2.01 ± 0.01 between the Control and the Experimental bioreactor, respectively, under the microaeration dose of 7.50 $mL_{O2}/L_{reactor}$–day in the Experimental bioreactor. A further increase was observed in the Experimental bioreactor from 2.01 ± 0.01 to 2.20 ± 0.00 as the microaeration dose increased from 7.50 to

15.0 $mL_{O2}/L_{reactor}$–day, while the Control bioreactor had no significant change. This change in the ratio could indicate a greater diversion of carbon mineralization towards CH_4, as hydrogenotrophic methanogenesis consumes CO_2. Thus, this change could have been a result of increase in the activity of hydrogenotrophic methanogens. This would be consistent with the observation that microaeration did not affect the yield of CH_4 from the destruction of VS while maintaining the solids removal efficiency. Furthermore, a reduction in the CO_2 fraction of the biogas brings down the cost of scrubbing the CO_2 for biogas reuse and improves the quality of fuel generated from the process.

Concentration of H_2S in the biogas decreased with continuous microaeration

During the AD process, sulfur compounds in the substrate, such as inorganic forms of sulfur, volatile organic sulfur compounds, as well as decay of sulfur-containing amino acids, are reduced to in biogas and sulfide (HS^- and S^{2-}) in the liquid phase. Sulfide in liquid phase is not only toxic to methanogens but also destructive to the AD system due to corrosive action on digester walls and pipes. Meanwhile, H_2S levels in the biogas can reach as high as 10,000 ppm. High concentration of odorous H_2S in biogas reduces its reuse potential and economic value and causes corrosion of concrete and steel pipeline (Chen et al., 2020). Thus, removal of H_2S from the biogas is an important step to prolong the life of the treatment infrastructure and for the reuse of biogas.

Microaeration has been demonstrated to allow up to 99% removal of H_2S from the biogas (Chen et al., 2020; Fu et al., 2023; Krayzelova et al., 2015; Nguyen and Khanal, 2018). The daily H_2S concentrations in the biogas from the Control bioreactor reached up to 4000 ppm. Microaeration of the methanogenic phase anaerobic digester reduced the daily concentration of H_2S in the biogas to as low as 80 ppm (Figure 15). Average values over long–

term operation reduced with an increase in microaeration doses and reaching as low as 220 ± 80 ppm under long term operation at 15.0 $mL_{O2}/L_{reactor}$–day, in the Experimental bioreactor.

Sulfate reducing bacteria (SRBs) produce H_2S and consume acetate and H_2 in the process (Krayzelova et al., 2015). The increase in the influence of hydrogenotrophic methanogens due to microaeration may lead to increase in the competition for H_2. Thus, one possible mechanism leading up to H_2S reduction could have been inhibition of the activity of SRBs due to competition for H_2 as a substrate. An investigation into the phylogenetic diversity of a thermophilic AD system treating municipal solid waste under microaeration, compared to the unaerated control, suggested that production of H_2S by SRBs was not suppressed due to microaeration despite measuring minimal H_2S in the biogas (Tang et al., 2004).

Initial exposure to microaeration led to rapid reduction of H_2S during preliminary tests and subsequent removal of the recirculation line resulted in rapid increase to even higher levels that prior to the start of tests (Figure 6A). This suggested that the reduction of H_2S in the biogas was a result of either activity of facultative aerobic microorganisms or an abiotic reaction due to the rapid response to both the addition as well as the removal of microaeration. Past investigations of the effect of microaeration on H_2S in a single stage AD system had reported similar trends in reduction and suggested that those reductions were microbially catalyzed by facultative organisms either along the walls of the headspace of the reactor or at the gas-liquid interphase (Chen et al., 2020; Fu et al., 2023; Krayzelova et al., 2015).

The concentration of H_2S in the biogas was also stabilized as the variation in the H_2S

levels went down with the increase in the oxygen dose (Figure 13). The relatively stable levels of H_2S, notwithstanding operational abnormalities, compared to the large variations in the H_2S concentrations in the Control bioreactor suggested that microaeration may assist in stabilizing the H_2S level in the biogas, and for a given AD system, microaeration could be deployed to control H_2S levels at discreet ranges. Conventional combustion engines for CHP generation require H_2S concentration as low as 100 ppm while the long-term operation under microaeration could only reach as low as 220 ± 80 ppm of H_2S in the biogas. While microaeration at the investigated doses may not be used as a standalone method of biogas desulfurization, it holds potential to be used in conjunction with order methods for biogas improvement and can supplement existing methods by reducing stress on those systems.

Sulfur transformations in a mesophilic anaerobic digester due to microaeration

This investigation demonstrated that microaeration in the methanogenic phase of a two-stage mesophilic anaerobic digestion process reduces the H_2S in the biogas collected from the digesters. To ensure that H_2S reduction from the biogas is non-recalcitrant, i.e., the H_2S is not converted to a form that may cause issues with downstream handling such as rapid and concentrated production H_2S in downstream biosolids handling, it is important to understand the nature of transformations that H_2S undergoes in an anaerobic digester with microaeration.

Various studies on the effect of varying dissolved oxygen (DO) during sulfide oxidation have concluded that the concentration of oxygen determines the final product of the process. Under microaerobic conditions, i.e., when the DO concentration is less than 0.1 mg/L, the main product of sulfide oxidation is elemental sulfur, while at higher DO concentrations, SO_4^{2-} is the final product. Roosta et al. (2011) evaluated the effect of sulfide

and DO concentrations on biological sulfide oxidation using *Thiobacillus thioparus* (DSMZ 5368) as the model sulfide oxidizing bacteria, and found that at the rate of sulfide oxidation to elemental sulfur was independent of DO except at very low levels, while rate of oxidation of sulfide to SO_4^{2-} increased with increased DO levels, thus at conditions that would prevail due to microaeration of anaerobic digestion, elemental sulfur would be expected as the main product of biological sulfide oxidation. Pokorna-Krayzelova et al. (2018) found that under limited-oxygen conditions, during both biochemical and chemical oxidation of sulfide, elemental sulfur (S^0) was the main product, accounting for 98.4% and over 99% of sulfide consumed, respectively, while SO_4^{2-} was the other product that was produced during their investigation.

The formation of S^0 due to microaeration was reported to impart a slight yellow color to the medium which is characteristic of elemental sulfur. Pokorna-Krayzelova et al. (2018) reported that there was difference in the appearance of S^0 depending on the mechanism by which it was produced – biologically produced S^0 appeared as yellowish flakes while the tests demonstrating chemical oxidation produced yellow suspensions. In this investigation, there was the formation of a white to light yellowish substances on the inner surface of the recirculation line of the Experimental bioreactor. Microaeration was applied to the Experimental bioreactor by using tubing with permeability towards oxygen for the recirculation line. Some sections of the recirculation line had tubing with higher permeability towards oxygen for the microaeration doses of 5.35 $mL_{O2}/L_{reactor}$–day and higher (Table 2). During the use of the higher permeability tubing, the deposition of the light-colored substance on the inner surface of the recirculation line was visibly higher (Figure 20). That had led to more frequent replacement of the tubing to maintain the intended dose of

microaeration for the Experimental bioreactor.

Figure 20. The development of flakes was observed on the recirculation line of the Experimental bioreactor during the use of higher permeability tubing to apply microaeration. (A) The section of the recirculation line with relatively lower permeability towards oxygen did not have a significant impact deposition of the white flakes, unlike (B) the section with higher permeability towards oxygen which had visible deposition of a white substance. Both the types of tubing were transparent, and the black color was due to the sludge flowing through them. These pictures were taken on July 11th, 2023, during the preliminary microaeration tests when the microaeration dose was 54.6 $mL_{O2}/L_{reactor}$–day for the Experimental bioreactor. Both the pictures were taken under similar lighting conditions.

Practical considerations and future research related to microaeration

This investigation demonstrated that microaeration in the methanogenic phase of a two-stage mesophilic anaerobic digestion process aids biogas desulfurization and does not adversely affect solids removal, under the conditions tested in this study. Microaeration is, thus, a valid and relatively low-cost method of biogas desulfurization.

Scaling this technology based on this investigation needs some practical considerations. The use of silicone tubing for microaeration during sludge recirculation is not scalable. The use of silicone tubing for passive diffusion of oxygen into the biomass has a higher oxygen transfer rate (OTR) than conventional aeration technologies (Li et al., 2023). This may lead to underestimation of the dose of oxygen that needs to be supplied for continuous microaeration due to the higher efficiency of the method used in this study.

Using bubble aerators also need the requirement of efficient mixing of the oxygen

within the AD system to avoid the need for over–aeration of the anaerobic community to match the OTR of the bubble-free method. Over–aeration has also been reported to lead to scaling due to excess sulfur deposition leading to clogging of pipelines (Krayzelova et al., 2015).

Microaeration has been used to control the H_2S in full-scale anaerobic digesters and to improve hydrolysis without adversely affecting the overall performance of the AD system (Krayzelova et al., 2015). The presence of oxygen presents various other opportunities in these systems such as the removal of other trace pollutants in the biogas. Ortiz-Ardila et al. (2024) found that microaeration could be used for the conversion of volatile siloxanes to methane and other simpler monomeric products.

do Nascimento et al. (2021) investigated the effect on microaeration on the removal/transformation of seven organic micropollutants and found that microaeration was an effective strategy for removal of the studied micropollutants in anaerobic wastewater treatment systems. Wei et al. (2024) found an increase in the filterability of sludge in an anerobic membrane bioreactor.

CONCLUSION

This study demonstrated that continuous microaeration in the methanogenic phase of a two-stage anaerobic digester, using bubble free supply of oxygen, can assist with biogas desulfurization. Consistent microaeration led to stabilization of H_2S levels in the biogas alongside reduction. There is evidence to suggest that there is no adverse effect of microaeration on neither the solids destruction efficiency nor the methane yield till a dose of 15.0 $mL_{O2}/L_{reactor}$–day. Furthermore, there was a possibility of microaeration shifting the dominance of methanogenic activity away from acetoclastic methanogenesis to hydrogenotrophic methanogenesis.

The use of bubble-free oxygen supply may lead to overestimation of an equivalent dose of oxygen that is delivered using bubbles, due to the potentially higher OTR of the bubble-free method. Thus, the doses tested in this study may correspond to higher doses while using delivering the oxygen using bubbles. Overall, this bench–scale study confirms that microaeration in the mesophilic methanogenic phase of a two-phased anaerobic digester can assist with biogas desulfurization and pilot–scale studies can be used for optimizing the doses while aerating the digesters with bubble-based methods.

APPENDIX

Table S1. Measurements of TS and VS in the feed and in the effluent of the Control (CB) and Experimental (EB) bioreactors.

Date	Feed		EB		CB	
	TS (%w/w)	VS (%w/w)	TS (%w/w)	VS (%w/w)	TS (%w/w)	VS (%w/w)
5/16/23	4.45	3.69	2.60	1.77	2.58	1.73
5/19/23	4.66	3.8	2.59	1.77	2.63	1.78
5/23/23	4.42	3.62	2.59	1.76	2.64	1.78
5/26/23	4.98	4.02	2.55	1.73	2.62	1.77
5/30/23			2.69	1.86	2.69	1.84
6/2/23	4.87	3.92	2.65	1.83	2.72	1.87
6/6/23	4.56	3.74	2.70	1.85	2.71	1.85
6/9/23	4.87	4.01	2.68	1.85	2.69	1.85
6/13/23	4.48	3.72	2.72	1.88	2.63	1.78
6/16/23	4.63	3.81	2.60	1.77	2.59	1.76
6/20/23	4.4	3.58	2.57	1.75	2.55	1.72
6/23/23	4.75	3.82	2.54	1.73	2.56	1.74
6/27/23	4.42	3.5	2.60	1.78	2.62	1.77
6/30/23	4.76	3.87	2.59	1.76	2.59	1.76
7/7/23	4.46	3.63	2.61	1.81	2.77	1.92
7/11/23	4.4	3.55	2.61	1.81	2.77	1.92
7/14/23	4.16	3.66	2.60	1.8	2.79	1.93
7/18/23	4.08	3.35	2.64	1.81	2.87	1.98
7/21/23	4.41	3.58	2.64	1.82	2.81	1.94
7/25/23	4.1	3.33	2.57	1.77	2.81	1.95
7/28/23	4.49	3.55	2.47	1.69	2.76	1.91
8/1/23	4.33	3.44	2.63	1.8	2.78	1.89
8/4/23	4.46	3.6	2.48	1.68	2.79	1.88
8/8/23	4.31	3.51	2.52	1.72	2.90	2.00
8/14/23	4.53	3.69	2.51	1.71	2.86	1.96
8/18/23	4.58	3.64	2.56	1.74	2.94	2.03
8/22/23	3.87	3.15	2.48	1.68	2.9	1.97
8/25/23	4.2	3.35	2.50	1.7	2.86	1.95
8/29/23	3.87	3.18	2.47	1.67	2.85	1.95
9/1/23	4.47	3.5	2.38	1.63	2.79	1.92
9/5/23	3.99	3.31	2.38	1.6	2.82	1.91

9/8/23	4.49	3.68	2.43	1.66	2.74	1.88
9/12/23	4.42	3.6	2.40	1.63	2.72	1.86
9/15/23	4.43	3.61	2.30	1.55	2.62	1.81
9/19/23	4.38	3.56	2.36	1.54	2.73	1.9
9/22/23	4.03	3.33	2.33	1.6	2.54	1.76
9/26/23	3.24	2.6	2.34	1.58	2.65	1.86
10/3/23	4.16	3.47	2.46	1.70	2.6	1.83
10/6/23	4.7	3.83	2.57	1.80	2.54	1.76
10/10/23	4.65	3.78			2.64	1.81
10/13/23	4.41	3.6	2.43	1.66	2.7	1.84
10/17/23	4.86	3.95	2.19	1.48	3.02	2.2
10/20/23	4.75	3.91	2.04	1.36	2.8	1.99
10/24/23	4.6	3.77	2.09	1.41	2.63	1.84
10/27/23	4.51	3.72	2.16	1.48	2.64	1.88
10/31/23	4.87	3.96	2.64	1.86	2.88	2.06
11/3/23	4.75	3.84	2.48	1.71	2.87	2.04
11/7/23	4.77	3.88	2.73	1.92	2.88	2.04
11/10/23	4.66	3.86	2.64	1.84	2.65	1.82
11/14/23	5.06	4.09	2.68	1.87	2.73	1.9
11/17/23	4.22	3.49	2.68	1.88	2.62	1.85
11/21/23	4.57	3.8	2.70	1.91	2.63	1.84
11/24/23	4.36	3.61	2.60	1.81	2.53	1.76
11/28/23	4.5	3.73	2.61	1.82	2.51	1.76
12/1/23	4.37	3.65	2.56	1.75	2.58	1.79
12/5/23	4.41	3.70	2.59	1.81	2.63	1.85
12/8/23	4.63	3.90	2.56	1.78	2.55	1.80
12/12/23	4.80	4.00	2.44	1.71	2.54	1.77
12/15/23	4.81	3.98	2.50	1.72	2.63	1.85
12/19/23	4.74	3.89	2.51	1.75	2.74	1.95
12/22/23	4.48	3.77	2.65	1.88	2.76	1.97
12/27/23	4.77	4.00	2.57	1.79	2.77	1.96
12/28/23	4.80	4.02	2.55	1.79	2.73	1.94
1/4/24	4.53	3.82	2.62	1.88	2.67	1.91
1/5/24	4.70	3.98	2.62	1.88	2.78	2.02
1/9/24	4.73	3.98	2.62	1.88	2.77	2.01
1/15/24	4.83	4.06	2.55	1.81	2.71	1.94
1/19/24	4.65	3.9	2.55	1.82	2.75	1.94
1/22/24	4.82	4.05	2.77	2.01	2.91	2.12

1/29/24	4.98	4.12	2.65	1.85	2.71	1.92
2/2/24	4.69	3.94	2.61	1.87	2.77	1.98
2/6/24	4.94	4.03	2.72	1.95	2.74	1.93
2/9/24	5.08	4.22	2.60	1.88	2.81	2.00
2/13/24	4.68	3.80	2.61	1.88	2.65	1.84
2/16/24	4.24	3.52	2.51	1.79	2.80	1.96
2/20/24	4.62	3.76	2.58	1.80	2.77	1.94
2/23/24	4.38	3.66	2.46	1.77	2.67	1.85
2/26/24	4.67	3.85	2.53	1.83	2.75	1.95
2/29/24	4.15	3.48	2.44	1.75	2.65	1.88
3/4/24	4.59	3.84	2.51	1.82	2.69	1.94
3/7/24	4.21	3.52	2.42	1.77	2.67	1.91
3/11/24	4.40	3.66	2.48	1.79	2.62	1.86
3/14/24	4.80	3.86	2.42	1.70	2.61	1.85
3/18/24	4.80	3.89	2.63	1.89	2.74	1.94
3/24/24	4.33	3.61	2.55	1.81	2.64	1.85
3/25/24	4.38	3.69	2.56	1.82	2.67	1.89
3/28/24	4.36	3.68	2.29	1.63	2.60	1.85
4/2/24	4.83	4.02	2.45	1.75	2.73	1.94
4/5/24	4.68	3.94	2.37	1.65	2.66	1.88
4/8/24	4.49	3.66	2.40	1.69	2.70	1.91
4/12/24	4.39	3.66	2.19	1.54	2.65	1.86
4/15/24	4.45	3.70	2.37	1.67	2.68	1.92
4/18/24	4.38	3.68	2.55	1.81	2.66	1.88
4/22/24	4.76	3.95	2.59	1.79	2.66	1.90
4/25/24	4.45	3.73	2.68	1.91	2.75	1.97
4/29/24	4.65	3.89	2.81	2.02	2.81	2.03
5/2/24	4.57	3.85	2.69	1.94	2.68	1.93
5/6/24	4.63	3.90	2.71	1.96	2.70	1.95
5/9/24	4.48	3.76	2.60	1.89	2.53	1.81
5/13/24	4.82	3.98	2.79	2.03	2.54	1.82
5/17/24			2.79	2.02	2.87	2.11
5/20/24	4.60	3.79	2.50	1.78	3.40	2.40
5/23/24	4.59	3.85	2.62	1.90	3.31	2.36
5/27/24	5.04	4.03	2.58	1.83	3.12	2.18
5/30/24	4.73	3.84	2.63	1.85	3.15	2.19
6/3/24	4.90	3.95	2.71	1.90	2.78	2.03
6/7/24	4.97	4.09	2.80	1.97	2.80	1.99

Table S2. Calculated total solids (TS) and volatile solids (VS) destruction efficiencies for the Experimental (EB) and the Control (CB) bioreactors.

Date	EB		CB	
	TS destruction (%)	VS destruction (%)	TS destruction (%)	VS destruction (%)
5/16/23	41.6	52.0	42.0	53.1
5/19/23	44.4	53.4	43.6	53.2
5/23/23	41.4	51.4	40.3	50.8
5/26/23	48.8	57.0	47.4	56.0
6/2/23	45.6	53.3	44.1	52.3
6/6/23	40.8	50.5	40.6	50.5
6/9/23	45.0	53.9	44.8	53.9
6/13/23	39.3	49.5	41.3	52.2
6/16/23	43.8	53.5	44.1	53.8
6/20/23	41.6	51.1	42.0	52.0
6/23/23	46.5	54.7	46.1	54.5
6/27/23	41.2	49.1	40.7	49.4
6/30/23	45.6	54.5	45.6	54.5
7/7/23	41.5	50.1	37.9	47.1
7/11/23	40.7	49.0	37.0	45.9
7/14/23	37.5	50.8	32.9	47.3
7/18/23	35.3	46.0	29.7	40.9
7/21/23	40.1	49.2	36.3	45.8
7/25/23	37.3	46.8	31.5	41.4
7/28/23	45.0	52.4	38.5	46.2
8/1/23	39.3	47.7	35.8	45.1
8/4/23	44.4	53.3	37.4	47.8
8/8/23	41.5	51.0	32.7	43.0
8/14/23	44.6	53.7	36.9	46.9
8/18/23	44.1	52.2	35.8	44.2
8/22/23	35.9	46.7	25.1	37.5
8/25/23	40.5	49.3	31.9	41.8
8/29/23	36.2	47.5	26.4	38.7
9/1/23	46.8	53.4	37.6	45.1
9/5/23	40.4	51.7	29.3	42.3
9/8/23	45.9	54.9	39.0	48.9
9/12/23	45.7	54.7	38.5	48.3

9/15/23	48.1	57.1	40.9	49.9
9/19/23	46.1	56.7	37.7	46.6
9/22/23	42.2	52.0	37.0	47.1
9/26/23	27.8	39.2	18.2	28.5
10/3/23	40.9	51.0	37.5	47.3
10/6/23	45.3	53.0	46.0	54.0
10/10/23			43.2	52.1
10/13/23	44.9	53.9	38.8	48.9
10/17/23	54.9	62.5	37.9	44.3
10/20/23	57.1	65.2	41.1	49.1
10/24/23	54.6	62.6	42.8	51.2
10/27/23	52.1	60.2	41.5	49.5
10/31/23	45.8	53.0	40.9	48.0
11/14/23	47.0	54.3	46.0	53.5
11/17/23	36.5	46.1	37.9	47.0
11/21/23	40.9	49.7	42.5	51.6
11/24/23	40.4	49.9	42.0	51.2
11/28/23	42.0	51.2	44.2	52.8
12/1/23	41.4	52.1	41.0	51.0
12/5/23	41.3	51.1	40.4	50.0
12/8/23	44.7	54.4	44.9	53.8
12/12/23	49.2	57.3	47.1	55.8
12/15/23	48.0	56.8	45.3	53.5
12/19/23	47.0	55.0	42.2	49.9
12/22/23	40.8	50.1	38.4	47.7
12/27/23	46.1	55.3	41.9	51.0
12/28/23	46.9	55.5	43.1	51.7
1/4/24	42.2	50.8	41.1	50.0
1/5/24	44.3	52.8	40.9	49.2
1/9/24	44.6	52.8	41.4	49.5
1/15/24	47.2	55.4	43.9	52.2
1/19/24	45.2	53.3	40.9	50.3
1/22/24	42.5	50.4	39.6	47.7
1/29/24	46.8	55.1	45.6	53.4
2/2/24	44.3	52.5	40.9	49.7
2/6/24	44.9	51.6	44.5	52.1
2/9/24	48.8	55.5	44.7	52.6
2/13/24	44.2	50.5	43.4	51.6

2/16/24	40.8	49.1	34.0	44.3
2/20/24	44.2	52.1	40.0	48.4
2/23/24	43.8	51.6	39.0	49.5
2/26/24	45.8	52.5	41.1	49.4
2/29/24	41.2	49.7	36.1	46.0
3/4/24	45.3	52.6	41.4	49.5
3/7/24	42.5	49.7	36.6	45.7
3/11/24	43.6	51.1	40.5	49.2
3/14/24	49.6	56.0	45.6	52.1
3/18/24	45.2	51.4	42.9	50.1
3/24/24	41.1	49.9	39.0	48.8
3/25/24	41.6	50.7	39.0	48.8
3/28/24	47.5	55.7	40.4	49.7
4/2/24	49.3	56.5	43.5	51.7
4/5/24	49.4	58.1	43.2	52.3
4/8/24	46.5	53.8	39.9	47.8
4/12/24	50.1	57.9	39.6	49.2
4/15/24	46.7	54.9	39.8	48.1
4/18/24	41.8	50.8	39.3	48.9
4/22/24	45.6	54.7	44.1	51.9
4/25/24	39.8	48.8	38.2	47.2
4/29/24	39.6	48.1	39.6	47.8
5/2/24	41.1	49.6	41.4	49.9
5/6/24	41.5	49.7	41.7	50.0
5/9/24	42.0	49.7	43.5	51.9
5/13/24	42.1	49.0	47.3	54.3
5/20/24	45.7	53.0	26.1	36.7
5/23/24	42.9	50.6	27.9	38.7
5/27/24	48.8	54.6	38.1	45.9
5/30/24	44.4	51.8	33.4	43.0
6/3/24	44.7	51.9	43.3	48.6
6/7/24	43.7	51.8	43.7	51.3
11/3/23	47.8	55.5	39.6	46.9
11/7/23	42.8	50.5	39.6	47.4
11/10/23	43.3	52.3	43.1	52.8

Table S3. Daily biogas production in the Experimental (EB) and the Control (CB) bioreactors, measured using the water displacement method.

Date	EB	CB
	L/day	L/day
5/14/23	2.09	1.86
5/15/23	2.28	1.97
5/16/23	2.38	2.28
5/17/23	2.33	1.95
5/18/23	2.35	2.09
5/19/23	2.26	2.20
5/20/23	1.85	1.75
5/21/23	2.23	2.18
5/22/23	2.19	2.15
5/23/23	2.34	2.15
5/24/23	2.03	1.81
5/25/23	2.18	1.70
5/26/23	2.12	1.83
5/27/23	2.41	2.34
5/28/23	2.38	2.18
5/29/23	2.52	2.20
5/30/23	2.39	1.14
5/31/23	2.10	2.02
6/1/23	1.98	
6/2/23	2.06	1.97
6/3/23	1.95	1.79
6/4/23	2.16	1.96
6/5/23	1.98	1.80
6/6/23	2.21	1.87
6/7/23	2.08	1.89
6/8/23	2.00	1.81
6/9/23	1.86	1.73
6/10/23	2.10	1.91
6/11/23	1.88	1.85
6/12/23	1.91	2.01
6/13/23	1.60	1.54
6/14/23	2.04	1.69
6/15/23	1.53	1.31
6/16/23	1.82	1.63
6/17/23	2.11	1.95

6/18/23	1.88	1.80
6/19/23	2.20	2.03
6/21/23	1.97	0.48
6/22/23	2.07	1.71
6/23/23	2.04	1.81
6/24/23	1.54	1.78
6/25/23	1.48	1.21
6/26/23	1.68	1.79
6/27/23	1.51	1.96
6/28/23	1.45	1.86
6/29/23	1.80	1.58
6/30/23	1.92	1.79
7/1/23	1.69	1.42
7/2/23		0.36
7/3/23	2.07	1.63
7/4/23	1.95	1.42
7/5/23	1.63	1.11
7/6/23	1.98	1.72
7/8/23	2.04	1.74
7/9/23	2.03	0.53
7/10/23	1.70	1.11
7/11/23	2.08	
7/12/23	1.72	1.59
7/13/23	1.78	
7/14/23	2.50	2.09
7/15/23	1.79	0.58
7/16/23	1.50	1.16
7/17/23	2.00	1.80
7/18/23	1.82	1.67
7/19/23	1.68	1.70
7/20/23	1.94	
7/21/23	1.84	1.66
7/23/23	1.16	1.03
7/24/23	1.75	1.68
7/25/23	1.72	1.66
7/26/23	2.04	0.80
7/27/23	1.72	1.39
7/28/23	1.78	0.39
7/29/23	1.88	0.61

7/30/23	1.69	1.24
7/31/23	1.74	0.92
8/1/23	1.79	1.69
8/2/23	1.60	1.55
8/3/23	1.54	1.34
8/4/23	1.50	1.44
8/5/23	1.49	1.39
8/6/23	1.75	1.63
8/12/23	1.43	0.37
8/14/23	1.38	0.60
8/15/23	1.63	0.64
8/16/23	0.99	0.89
8/17/23	1.47	0.93
8/18/23	1.79	1.13
8/19/23	1.78	0.98
8/20/23	2.53	
8/22/23	2.60	2.07
8/23/23	0.63	0.31
8/24/23	1.07	0.36
8/25/23	1.62	
8/26/23	1.85	1.15
8/27/23	2.01	0.97
8/28/23	0.27	
8/29/23	2.03	1.55
8/30/23	1.68	0.29
8/31/23	1.44	1.04
9/1/23	1.15	0.22
9/3/23	0.16	0.10
9/4/23	1.62	
9/5/23	1.11	
9/6/23	1.35	
9/7/23	1.12	
9/10/23	1.18	1.13
9/12/23	1.70	1.51
9/13/23	0.75	0.80
9/14/23	1.84	0.97
9/15/23	0.34	1.49
9/16/23	0.21	1.45
9/17/23	2.11	2.00

9/19/23	1.99	
9/22/23	0.73	1.50
9/25/23	1.70	1.49
9/26/23	2.02	1.65
9/28/23	1.23	0.82
9/29/23	1.71	1.15
9/30/23	1.82	0.61
10/1/23	1.95	1.62
10/2/23	1.81	1.82
10/3/23	2.62	1.69
10/4/23	3.43	1.74
10/5/23		1.38
10/6/23	1.46	0.28
10/7/23	0.62	1.61
10/9/23	1.20	1.57
10/10/23	2.95	2.06
10/13/23	0.47	0.29
10/14/23	1.40	1.38
10/15/23	0.81	0.82
10/16/23	1.51	0.55
10/17/23	0.52	1.96
10/19/23	0.14	0.59

Table S4. Daily biogas production in the Experimental (EB) and the Control (CB) bioreactors, measured using the respirometer.

Date	EB	CB
	L/day	L/day
10/20/23	0.48	1.49
10/21/23	0.87	0.27
10/22/23	0.99	1.30
10/23/23	2.09	2.45
10/24/23	0.74	
10/26/23	0.63	
10/27/23	0.92	
10/28/23	0.77	
10/29/23	1.00	
10/30/23	1.29	
10/31/23	0.46	
11/1/23	1.33	0.51
11/2/23	1.27	0.52
11/3/23	1.33	1.31
11/4/23	1.28	0.62
11/6/23	1.23	0.18
11/7/23	1.46	1.43
11/8/23	1.69	1.01
11/9/23	1.15	0.73
11/10/23		1.30
11/13/23	1.36	1.07
11/14/23	2.07	1.52
11/15/23	1.41	1.62
11/17/23	1.19	0.20
11/18/23	1.38	
11/19/23	1.31	
11/20/23	1.24	1.10
11/21/23	1.44	1.63
11/23/23	1.14	0.76
11/24/23	1.16	0.68
11/26/23	0.86	0.46
11/27/23	1.47	1.07
11/28/23	1.26	0.84
11/29/23	0.85	
11/30/23	1.70	0.74

12/1/23	1.20	0.21
12/2/23	1.27	0.73
12/4/23	1.22	0.77
12/5/23	1.29	0.77
12/6/23	1.23	0.88
12/7/23	3.09	1.58
12/8/23	1.82	1.49
12/9/23	2.37	0.83
12/10/23	1.93	
12/11/23	1.86	1.01
12/12/23	2.12	0.80
12/13/23	1.77	0.49
12/14/23	2.25	
12/15/23	1.83	0.81
12/16/23	2.22	0.55
12/17/23	2.00	0.86
12/18/23	1.92	1.19
12/19/23	1.92	0.79
12/20/23	1.82	1.06
12/21/23	1.70	0.84
12/22/23	2.10	0.98
12/26/23	2.53	0.14
12/27/23	2.32	1.47
12/28/23	2.90	1.22
12/29/23	1.89	1.03
12/30/23	1.98	1.24
12/31/23	1.59	0.85
1/1/24	1.75	0.75
1/2/24	1.61	0.58
1/3/24	1.50	0.88
1/4/24	1.84	0.67
1/5/24	1.48	0.78
1/6/24	1.62	1.00
1/7/24	1.54	1.37
1/8/24	1.72	1.72
1/9/24	1.83	1.34
1/10/24	1.97	1.21
1/11/24	1.53	0.87
1/12/24	1.85	1.49

1/13/24		1.17
1/14/24	2.06	1.92
1/15/24	1.71	0.72
1/16/24	1.99	1.27
1/17/24	1.35	1.19
1/18/24	2.05	1.53
1/19/24	1.81	1.62
1/20/24	1.70	1.55
1/21/24	1.59	1.47
1/22/24	2.51	1.98
1/23/24	1.96	1.72
1/24/24	2.06	1.70
1/25/24	2.34	2.16
1/26/24	2.54	1.55
1/27/24	2.26	1.49
1/28/24	1.93	1.02
1/29/24	1.04	1.57
1/30/24	2.96	1.60
1/31/24	1.36	2.23
2/1/24	2.29	1.72
2/2/24	1.87	1.42
2/3/24	2.73	1.50
2/4/24	1.50	1.22
2/5/24	2.42	1.12
2/6/24	1.35	
2/7/24	2.29	1.20
2/8/24	1.99	1.90
2/9/24	2.47	1.93
2/10/24	1.70	1.57
2/11/24	2.26	0.77
2/12/24	1.72	
2/13/24	1.80	1.67
2/14/24	2.45	1.56
2/15/24	1.73	2.27
2/16/24	1.83	1.64
2/17/24	1.93	2.52
2/18/24	1.44	1.57
2/19/24	1.44	1.31
2/20/24	1.78	1.57

2/21/24	1.87	
2/22/24	2.02	1.65
2/23/24	1.92	1.34
2/24/24	2.01	
2/25/24	1.71	1.22
2/26/24	2.11	0.88
2/27/24	1.83	1.25
2/28/24	2.55	1.78
2/29/24	1.34	0.84
3/1/24	1.74	1.82
3/2/24	1.76	1.52
3/3/24	1.97	1.08
3/4/24	2.13	2.55
3/5/24	1.63	1.06
3/6/24	2.11	1.92
3/7/24	1.74	1.90
3/8/24	1.86	2.00
3/9/24	2.50	1.53
3/10/24	2.33	1.89
3/11/24	1.90	0.88
3/12/24	1.88	0.89
3/13/24	1.92	1.74
3/14/24	0.00	0.90
3/15/24	2.16	1.94
3/16/24	2.04	0.91
3/17/24	2.43	0.73
3/18/24	2.14	0.95
3/19/24	1.99	0.78
3/20/24	2.11	
3/23/24	2.50	2.46
3/24/24	1.12	1.19
3/25/24	1.34	0.96
3/26/24	1.76	0.85
3/27/24	2.30	
3/28/24	1.40	1.90
3/29/24	1.92	1.76
3/30/24	2.48	
3/31/24	1.98	1.84
4/1/24	2.42	2.42

4/2/24	1.31	2.55
4/3/24	1.77	
4/4/24	2.10	3.38
4/5/24	2.37	2.47
4/6/24	1.84	2.85
4/7/24	1.87	1.36
4/8/24	1.81	1.49
4/9/24	1.82	1.31
4/10/24	1.93	1.11
4/11/24	1.96	1.25
4/12/24	1.21	1.66
4/13/24	1.99	1.50
4/14/24	2.06	1.40
4/15/24	1.88	1.42
4/16/24	1.86	2.42
4/17/24	2.57	1.93
4/18/24	2.21	2.02
4/19/24	2.09	1.62
4/20/24	1.95	0.94
4/21/24	2.33	1.42
4/22/24	2.24	1.46
4/23/24	2.29	
4/24/24	2.61	1.84
4/25/24	2.18	1.41
4/26/24	2.31	1.68
4/27/24	2.29	1.84
4/28/24	2.78	1.56
4/29/24	2.12	1.49
4/30/24	2.17	1.63
5/1/24	2.21	1.60
5/2/24	2.04	1.41
5/3/24	2.64	1.36
5/4/24	2.59	2.26
5/5/24	2.61	2.57
5/6/24	1.49	2.10
5/7/24	1.83	2.35
5/8/24	1.90	1.33
5/9/24	1.96	1.85
5/10/24	2.41	1.30

5/11/24	2.19	1.83
5/12/24	2.31	1.63
5/13/24	2.00	1.49
5/14/24	1.91	1.38
5/16/24	2.52	1.80
5/17/24	2.61	1.09
5/18/24	2.06	1.46
5/19/24	1.85	1.46
5/20/24	2.53	1.16
5/21/24	1.93	1.84
5/22/24	1.94	1.97
5/23/24	1.95	2.45
5/24/24	2.03	2.34
5/25/24	2.21	1.60
5/26/24	2.14	1.44
5/27/24	2.01	2.44
5/28/24	1.88	1.62
5/29/24	2.01	1.39
5/30/24	2.63	0.76
5/31/24	2.21	1.64
6/1/24	1.60	1.16
6/2/24	1.48	1.33
6/3/24	1.84	1.96
6/4/24	1.56	1.92
6/5/24	1.75	2.45
6/6/24	1.65	1.70
6/7/24	2.86	0.81

Table S5. Calculated methane Yield for Control (CB) and Experimental (EB) bioreactors when the water displacement method was used for biogas production measurement and the GC method was used for methane concentration measurements.

Date	CB	EB	CB		EB	
	L_{CH4}/day	L_{CH4}/day	$g_{VSremoved}$/day	$L_{CH4}/g_{VSremoved}$	$g_{VSremoved}$/day	$L_{CH4}/g_{VSremoved}$
5/19/23	1.33	1.28	1.62	0.82	0.97	1.32
5/23/23	1.36	1.33	1.47	0.93	0.82	1.61
5/26/23	1.13	1.30	1.80	0.63	1.18	1.10
6/2/23	1.12	1.18	1.64	0.68	1.02	1.16
6/6/23	1.04	1.20	1.51	0.69	0.83	1.44
6/9/23	0.98	1.15	1.73	0.57	1.06	1.08
6/13/23		1.18	1.55		0.80	1.47
6/16/23	0.89	1.12	1.64	0.54	0.97	1.16
6/20/23	1.08	1.29	1.49	0.73	0.81	1.59
6/23/23	1.02	1.17	1.66	0.62	1.02	1.14
6/27/23	1.12	0.92	1.38	0.81	0.72	1.28
6/30/23	1.04	1.21	1.69	0.62	1.02	1.18
7/7/23	0.96	1.19	1.37	0.70	0.82	1.46
7/11/23	1.02	1.26	1.30	0.78	0.75	1.68
7/14/23	1.26	1.49	1.38	0.91	0.85	1.76
7/18/23	1.04	1.15	1.10	0.95	0.57	2.02
7/21/23	1.07	1.15	1.31	0.82	0.75	1.53
7/25/23		1.11	1.10		0.61	1.83
8/1/23	1.02	1.20	1.24	0.82	0.65	1.85
8/4/23	0.87	0.94	1.38	0.63	0.90	1.05
8/8/23		1.75	1.21		0.79	2.21
8/14/23	0.36	0.88	1.38	0.26	0.94	0.93
8/18/23		1.04	1.29		0.86	1.20
8/25/23		1.01	1.12		0.68	1.48
8/29/23	0.94	1.33	0.98	0.95	0.57	2.34
9/1/23	0.13	0.80	1.26	0.10	0.90	0.89
9/5/23		0.78	1.12		0.74	1.05
9/8/23		0.81	1.44		1.00	0.81
9/12/23	1.11	1.12	1.39	0.79	0.96	1.16
9/15/23	1.00	0.09	1.44	0.70	1.05	0.09
9/19/23	1.02	1.35	1.33	0.77	0.96	1.41
9/22/23	0.99	0.47	1.26	0.78	0.80	0.58
9/26/23		1.17	0.59		0.21	5.64

10/6/23		0.03	1.66		1.01	0.03
10/17/23	1.08	0.30	1.40	0.77	1.41	0.21

Table S6. Calculated methane Yield for the Experimental (EB) and the Control (CB) bioreactors when the respirometer was used for biogas production measurements and the GC method was used for methane concentration measurements.

Date	CB	EB	CB		EB	
	L_{CH4}/day	L_{CH4}/day	$g_{VSremoved}$/day	$L_{CH4}/g_{VSremoved}$	$g_{VSremoved}$/day	$L_{CH4}/g_{VSremoved}$
10/20/23	1.16	0.96	1.54	0.76	1.50	0.64
10/24/23	1.15	1.20	1.54	0.74	1.34	0.90
10/27/23	1.01	0.57	1.47	0.68	1.25	0.46
10/31/23	1.02	1.48	1.52	0.67	1.06	1.40
11/3/23		0.86	1.44		1.09	0.79
11/7/23	0.19	1.17	1.47	0.13	0.92	1.27
11/10/23	0.82	1.12	1.63	0.50	0.98	1.15
11/14/23	0.83	1.22	1.75	0.47	1.13	1.08
11/17/23		0.88	1.31		0.65	1.35
11/21/23	0.18	1.28	1.57	0.12	0.88	1.46
11/24/23	0.81	0.90	1.48	0.54	0.81	1.11
11/28/23	0.72	0.97	1.58	0.46	0.90	1.09
12/1/23		0.95	1.49		0.87	1.09
12/5/23	0.56	0.87	1.48	0.38	0.89	0.98
12/8/23		1.37	1.68		1.07	1.28

Table S7. Calculated methane yield from VS destruction in CB and EB (using respirometer for biogas production measurement and MRU Optimax for gas composition analysis).

Date	CB	EB	CB		EB	
	L_{CH4}/day	L_{CH4}/day	$g_{VSremoved}$/day	$L_{CH4}/g_{VSremoved}$	$g_{VSremoved}$/day	$L_{CH4}/g_{VSremoved}$
1/4/24	0.24	1.22	1.53	0.16	0.96	1.27
1/9/24	0.85	1.22	1.58	0.54	1.09	1.12
1/15/24		1.32	1.70		1.21	1.09
1/19/24	1.03	1.18	1.57	0.66	1.08	1.09
1/22/24	1.25	1.63	1.54	0.81	1.02	1.60
1/29/24	0.86	0.63	1.76	0.49	1.18	0.53
2/2/24	0.87	1.08	1.57	0.55	1.06	1.02
2/6/24		0.87	1.68		1.05	0.83
2/9/24	1.22	1.59	1.78	0.68	1.30	1.23
2/13/24		1.18	1.57		0.95	1.24
2/16/24	1.06	1.21	1.25	0.85	0.81	1.50
2/20/24	0.96	1.14	1.46	0.66	0.94	1.21
2/23/24	0.80	1.19	1.45	0.55	0.96	1.24
2/26/24	0.56	1.30	1.52	0.37	1.06	1.23
2/29/24		0.89	1.28		0.83	1.07
3/4/24	1.59	1.33	1.52	1.05	1.06	1.25
3/11/24	0.56	1.24	1.44	0.39	0.94	1.31
3/14/24	0.57	1.21	1.61	0.35	1.15	1.05
3/18/24	0.61	1.41	1.56	0.39	1.01	1.40
3/24/24	0.74	0.72	1.41	0.53	0.85	0.85
3/25/24	0.58		1.44	0.40	0.90	
3/28/24	1.20	0.92	1.46	0.82	1.11	0.83
4/2/24	1.64	0.88	1.66	0.98	1.26	0.70
4/5/24	1.56	1.59	1.65	0.95	1.26	1.27
4/8/24	0.94	1.21	1.40	0.67	1.01	1.20
4/12/24	1.05	0.80	1.44	0.73	1.18	0.68
4/15/24	0.90	1.25	1.42	0.63	1.06	1.18
4/18/24	1.28	1.49	1.44	0.89	0.90	1.65
4/22/24	0.92	1.49	1.64	0.56	1.09	1.37
4/25/24	0.90	1.44	1.41	0.64	0.84	1.71
4/29/24	0.89	1.41	1.49	0.60	0.86	1.63
5/2/24	0.89	1.36	1.54	0.58	0.93	1.46
5/6/24	1.30	0.79	1.56	0.83	0.95	0.83
5/9/24	1.16	1.29	1.56	0.74	0.93	1.39

5/13/24	0.93	1.24	1.73	0.54	0.95	1.31
5/20/24	0.72	1.62	1.11	0.65	1.03	1.57
5/23/24	1.53	1.30	1.19	1.29	0.98	1.32
5/27/24	1.53	1.31	1.48	1.04	1.16	1.13
5/30/24	0.48	1.13	1.32	0.37	0.97	1.17
6/3/24	1.24	1.22	1.54	0.81	0.99	1.23
6/7/24	0.52	1.69	1.68	0.31	1.03	1.64

Table S8. H_2S concentration in the collected biogas in reactors EB and CB using Acrulog handheld gas composition analyzer

Date	EB	CB
	ppm	ppm
5/15/23	197	66
5/16/23	508	113
5/17/23	479	89
5/18/23	583	56
5/19/23	526	56
5/20/23	606	94
5/21/23	672	38
5/22/23	700	42
5/23/23	611	19
5/27/23	710	14
5/28/23	743	24
5/29/23	682	19
5/30/23	747	24
5/31/23	658	28
6/1/23	710	
6/2/23	700	28
6/3/23	761	9
6/4/23	710	33
6/5/23	813	33
6/6/23	804	24
6/7/23	597	9
6/8/23	747	19
6/9/23	743	14
6/10/23	776	24
6/11/23	771	33
6/12/23	606	5
6/13/23	400	33
6/14/23	82	47
6/15/23	160	38
6/16/23	649	9
6/17/23	851	5
6/18/23	949	56
6/19/23	771	42

6/20/23	907	38
6/21/23	926	5
6/22/23	1006	19
6/23/23	841	14
6/24/23	287	5
6/25/23	150	5
6/26/23	315	9
6/27/23	301	14
6/28/23	226	14
6/29/23	442	19
6/30/23	616	5
7/1/23	780	24
7/2/23	724	24
7/3/23	776	24
7/4/23	921	28
7/5/23	898	28
7/6/23	907	75
7/8/23	860	61
7/9/23	776	38
7/10/23	729	24
7/11/23	677	19
7/12/23	545	52
7/13/23	254	
7/14/23	324	75
7/15/23	287	75
7/16/23	263	165
7/17/23	301	226
7/18/23	216	254
7/19/23	179	202
7/20/23	118	
7/21/23	85	235
7/23/23	362	122
7/24/23	512	94
7/25/23	573	108
7/26/23	404	61
7/27/23	357	132
7/28/23	338	99
7/29/23	343	75
7/30/23	334	108

7/31/23	287	85
8/1/23	273	103
8/2/23	244	80
8/3/23	221	127
8/4/23	207	94
8/5/23	226	56
8/6/23	226	47
8/7/23	165	75
8/8/23	226	75
8/9/23	193	42
8/10/23	212	38
8/12/23	188	42
8/14/23	197	42
8/15/23	287	56
8/16/23		61
8/17/23	348	75
8/18/23	310	108
8/19/23	334	127
8/20/23	385	
8/21/23	395	230
8/22/23	353	268
8/23/23	301	108
8/25/23	381	160
8/26/23	409	113
8/27/23	118	132
8/28/23	85	108
8/29/23	301	160
8/30/23	334	89
8/31/23	475	179
9/1/23	461	188
9/2/23	89	179
9/3/23	141	33
9/4/23	432	
9/5/23	564	71
9/6/23		14
9/7/23	470	
9/8/23	508	5
9/10/23	367	179
9/12/23	588	179

9/13/23	620	108
9/14/23	719	183
9/15/23	517	230
9/16/23	512	19
9/17/23	526	136
9/22/23	517	451
9/25/23	517	719
9/25/23		
9/26/23	428	522
9/28/23	296	221
9/29/23	428	136
9/30/23	484	132
10/1/23	550	122
10/2/23	536	136
10/3/23	28	179
10/4/23	0	193
10/5/23	0	197
10/6/23	0	273
10/7/23	188	329
10/9/23	1194	353
10/10/23	169	348
10/12/23	376	291
10/13/23	385	291
10/14/23	432	564
10/15/23	644	348
10/16/23	338	667
10/17/23	362	235
10/19/23	320	423
10/20/23	193	437
10/21/23	188	301
10/22/23	306	465
10/23/23	729	1048
10/24/23	630	1763
10/25/23	639	1791
10/26/23		1777
10/27/23	691	1368
10/28/23	658	1387
10/29/23	761	1293
10/30/23	757	1250

10/31/23	484	790
11/1/23	484	550
11/2/23	432	498
11/3/23	639	414
11/4/23	635	
11/5/23	573	169
11/6/23	588	136
11/7/23	432	155
11/8/23	395	80
11/9/23	451	85
11/10/23	432	179
11/11/23		197
11/12/23	569	320
11/13/23	545	287
11/14/23	465	597
11/15/23	465	531
11/16/23	432	85
11/17/23	414	14
11/18/23	503	33
11/19/23	291	42
11/20/23	583	291
11/21/23	550	1043
11/23/23	484	1090
11/24/23	447	536
11/26/23	470	635
11/27/23	475	978
11/28/23	447	592
11/29/23	447	
11/30/23	489	470
12/1/23	508	254
12/2/23		367
12/4/23	489	559
12/5/23		461
12/7/23	508	268
12/9/23	409	
12/11/23	508	526
12/12/23	550	573
12/13/23	484	357
12/14/23	432	179

12/17/23	470	447
12/18/23	494	573
12/19/23	338	479
12/23/23	620	508
12/25/23	583	324
12/26/23	583	324
12/29/23	597	682
12/30/23	729	432
12/31/23	757	385
1/1/24	714	442
1/2/24	776	729

Table S9. H_2S concentration in the collected biogas in reactors EB and CB using MRU Instruments handheld gas composition analyzer.

Date	Methane		CO_2		O_2		H_2S	
	CB	EB	CB	EB	CB	EB	CB	EB
	%	%	%	%	%	%	ppm	ppm
1/3/24	66.4	66.4	30.8	30.9	0.73	0.62	852	976
1/5/24	36.0	66.6	19.5	29.7	0.69	0.94	1031	963
1/6/24	65.5	65.8	31.4	31.3	0.68	0.56	869	972
1/7/24	63.4	66.4	32.8	30.4	0.46	0.49	612	877
1/8/24	63.7	66.5	33.8	30.8	0.09	0.41	621	763
1/9/24	63.3	66.5	34.3	31.1	0.09	0.39	736	755
1/10/24	64.1	66.2	33.4	31.3	0.43	0.29	967	733
1/11/24	64.9	66.6	33.3	30.7	0.39	0.32	1008	709
1/12/24	64.9	67.0	33.5	30.5	0.30	0.27	1062	678
1/13/24	64.4	72.4	34.6	24.7	0.23	0.40	1134	467
1/14/24		63.9		33.6		0.30		710
1/16/24	63.7	64.7	34.6	31.7	0.12	0.32	1073	644
1/17/24	64.4	65.5	34.4	32.1	0.20	0.15	1053	676
1/18/24	63.0	65.3	34.2	32.6	0.24	0.19	1090	705
1/19/24	63.7	65.2	34.1	32.9	0.25	0.05	782	729
1/20/24	63.6	66.0	34.9	32.1	0.27	0.21	996	674
1/21/24	53.8	64.2	29.5	32.9	3.28	0.13	760	795
1/22/24	63.0	65.0	35.1	32.0	0.25	0.27	795	730
1/23/24	56.0	62.6	31.0	31.5	2.17	0.16	461	728
1/24/24	63.2	63.4	35.1	32.1	0.20	0.19	611	733
1/25/24		65.0		32.9		0.21		745
1/26/24	62.4	65.1	34.5	32.8	0.36	0.18	685	710
1/27/24	63.8	63.1	31.6	35.1	0.65	0.21	733	701
1/28/24	63.3	63.6	35.1	32.3	0.31	0.25	718	328
1/29/24	54.9	60.1	30.3	31.9	3.76	0.11	514	227
1/30/24	63.2	57.8	35.2	30.2	0.18	1.17	717	482
1/31/24	55.6		30.1		3.32		427	
2/1/24	63.7	61.1	34.1	31.7	0.25	0.28	782	234
2/2/24	61.1	57.6	33.9	31.3	0.22	0.20	840	309
2/3/24	63.8	62.6	35.1	31.6	0.12	0.13	883	593
2/4/24	63.4	60.5	34.9	32.1	0.25	0.08	840	549
2/5/24	62.0		34.0		0.79		807	
2/6/24	62.9	64.1	35.5	31.8	0.17	0.54	891	916
2/7/24	63.1	63.4	34.8	31.9	0.14	0.52	718	812

2/8/24	64.0	65.4	34.6	32.5	0.16	0.14	781	750
2/9/24	63.0	64.4	35.1	33.0	0.18	0.18	826	738
2/10/24	63.3	64.9	34.6	32.2	0.35	0.25	837	658
2/11/24	63.2	64.2	34.4	32.0	0.20	0.39	823	557
2/12/24	63.0	65.6	35.9	32.0	0.59	0.20	694	472
2/13/24		65.7		32.0		0.15		423
2/14/24	63.8	64.1	34.9	32.2	0.15	0.12	601	379
2/15/24	63.7	64.9	35.0	32.2	0.11	0.20	647	376
2/16/24	64.3	66.0	35.2	32.9	0.23	0.10	699	399
2/17/24	63.4	66.0	34.9	32.0	0.29	0.15	733	329
2/18/24	62.9	64.2	35.1	33.8	0.29	0.13	782	310
2/19/24	63.4	63.5	34.3	34.4	0.36	0.24	771	447
2/20/24	61.0	64.2	32.9	34.2	1.40	0.15	794	503
2/21/24		64.4		33.5		0.09		485
2/22/24	62.5	64.9	34.7	32.8	0.16	0.11	472	431
2/23/24	59.8	62.2	34.0	32.0	0.23	0.09	720	448
2/24/24		65.0		32.8		0.22		455
2/25/24	63.3	64.6	35.1	32.3	0.26	0.20	766	465
2/26/24	63.4	61.4	34.5	30.5	0.38	0.38	734	460
2/27/24	63.3	64.5	35.2	32.4	0.15	0.17	923	470
2/28/24	62.7	64.2	35.1	32.4	0.20	0.15	1022	482
2/29/24		66.4		32.0		0.13		476
3/1/24	62.7	65.2	35.1	33.1	0.13	0.12	1186	506
3/2/24	62.9	64.4	35.1	32.6	0.32	0.17	1080	478
3/3/24	62.9	64.3	35.2	32.9	0.26	0.10	1192	481
3/4/24	62.5	62.5	34.7	30.8	0.32	0.16	915	443
3/5/24	62.9	64.6	35.3	32.7	0.09	0.06	1142	463
3/6/24	62.7	64.8	35.1	32.4	0.14	0.14	470	470
3/7/24	63.6	65.8	35.0	32.1	0.07	0.14	1209	473
3/8/24	62.2	64.5	35.2	32.6	0.18	0.18	481	481
3/9/24	60.7	64.3	34.3	32.2	0.52	0.19	1085	484
3/10/24	62.4	62.5	35.2	31.2	0.19	0.13	831	512
3/11/24	63.4	65.4	34.9	32.2	0.22	0.13	1154	524
3/12/24	60.6	65.0	33.6	32.3	0.99	0.09	1170	546
3/13/24	62.6	63.4	35.5	31.4	0.21	0.70	1269	531
3/14/24	63.1	64.7	35.5	32.2	0.18	0.10	1339	528
3/15/24	63.4	64.2	35.2	32.8	0.29	0.17	1319	402
3/16/24	63.2	64.1	34.4	32.7	0.42	0.14	1287	504
3/17/24		65.0		32.6		0.23		496

3/18/24	64.0	66.0	34.9	32.1	0.30	0.12	1397	515
3/19/24		66.1		32.1		0.12		515
3/20/24	63.6	65.6	35.2	32.4	0.11	0.12	1440	525
3/22/24	62.1	62.5	35.2	34.5	0.23	0.12	941	526
3/23/24		46.5		23.6		1.67		465
3/24/24	62.6	64.4	35.0	32.4	0.23	0.14	1265	542
3/25/24	60.3		33.7		1.21		954	
3/26/24		64.9		30.8		0.13		490
3/27/24		62.3		28.2		0.21		466
3/28/24	63.4	65.9	32.5	29.1	0.23	0.21	1038	441
3/29/24	61.7	66.6	33.8	29.1	0.18	0.16	1078	415
3/30/24		66.5		29.5		0.22		425
3/31/24	63.9	66.8	34.3	29.7	0.13	0.10	746	430
4/1/24	63.3	63.3	34.6	28.5	0.20	0.11	1004	420
4/2/24	64.2	66.9	34.6	29.6	0.19	0.15	1020	408
4/3/24		66.3		30.0		0.08		415
4/4/24	63.2	66.8	33.7	29.2	0.34	0.09	449	403
4/5/24	63.3	67.2	34.6	29.2	0.16	0.12	751	399
4/6/24	63.7	67.1	34.5	29.4	0.15	0.12	851	407
4/7/24	62.2	66.2	34.1	29.2	0.54	0.38	711	379
4/8/24	63.2	66.6	34.2	29.8	0.19	0.10	738	390
4/9/24	63.2	66.1	33.9	29.4	0.15	0.32	606	350
4/10/24	64.3	66.2	34.3	29.6	0.16	0.31	707	359
4/11/24	62.6	65.9	34.5	29.8	0.36	0.32	449	348
4/12/24	63.5	66.5	35.4	30.7	0.12	0.11	668	359
4/13/24	62.6	64.7	34.3	29.6	0.47	0.46	405	294
4/14/24	62.2	65.1	34.7	30.0	0.22	0.10	351	299
4/15/24	63.1	66.7	34.6	29.8	0.22	0.13	349	321
4/16/24	61.9	65.9	34.1	29.6	0.17	0.11	322	300
4/17/24	62.4	66.3	35.0	30.0	0.14	0.09	521	360
4/18/24	63.6	67.5	34.6	29.5	0.12	0.05	481	353
4/19/24	60.2	67.3	32.5	29.9	0.23	0.11	570	358
4/20/24	64.5	67.1	34.1	28.8	0.27	0.20	569	344
4/21/24	62.4	67.1	34.6	29.6	0.18	0.13	370	366
4/22/24	63.1	66.7	34.6	29.8	0.23	0.14	368	328
4/23/24	62.2	65.6	31.3	29.8	0.59	0.14	293	327
4/24/24	62.3	66.3	34.8	30.4	0.15	0.10	346	375
4/25/24	64.1	66.0	34.9	30.2	0.11	0.08	515	306
4/26/24	62.3	65.9	34.1	30.5	0.46	0.05	568	339

4/27/24	62.6	60.1	34.5	27.2	0.34	0.35	308	335
4/28/24	60.5	64.9	33.0	29.4	0.17	0.23	572	334
4/29/24	59.6	66.5	32.1	29.8	1.51	0.14	391	331
4/30/24	63.6	66.5	35.0	29.9	0.16	0.11	601	339
5/1/24	62.1	67.8	34.2	29.9	0.73	0.09	569	350
5/2/24	63.0	66.5	35.0	30.1	0.18	0.07	402	354
5/3/24	62.8	64.9	35.0	30.9	0.24	0.12	491	260
5/4/24	62.3	58.6	35.0	30.9	0.21	0.22	383	128
5/5/24	63.5	56.2	34.8	31.8	0.16	0.10	604	87
5/6/24	61.8	52.8	35.2	29.2	0.29	0.32	658	150
5/7/24	63.6	63.0	34.6	32.5	0.13	0.09	786	376
5/8/24	62.9	64.7	35.4	31.4	0.10	0.04	875	513
5/9/24	62.8	65.8	35.5	30.5	0.10	0.07	881	485
5/10/24	63.9	65.9	34.1	30.6	0.23	0.08	942	465
5/11/24	62.5	65.8	34.7	30.3	0.19	0.11	989	355
5/12/24	61.5	61.7	34.6	30.5	0.06	0.02	1279	284
5/13/24	62.2	62.2	35.3	30.9	0.12	0.10	1291	452
5/14/24	61.9	61.9	35.3	30.5	0.13	0.09	1279	432
5/16/24	62.3	54.7	34.1	30.5	0.17	0.44	1572	140
5/17/24	62.5	33.1	34.6	28.6	0.35	0.44	2107	13
5/18/24	62.4	43.5	34.7	28.4	0.13	0.10	2514	182
5/19/24	61.9	59.6	35.9	29.4	0.03	0.08	3209	496
5/20/24	62.1	64.2	35.3	29.7	0.13	0.09	4170	651
5/21/24	62.6	65.6	35.5	29.7	0.07	0.07	4993	632
5/22/24	62.0	66.2	35.8	29.9	0.07	0.09	5451	627
5/23/24	62.6	66.7	35.1	29.2	0.05	0.08	5548	586
5/24/24	61.2	66.4	33.8	29.0	0.81	0.13	5295	439
5/25/24	63.0	61.3	35.3	30.0	0.08	0.10	5476	271
5/26/24	62.9	64.5	35.3	29.8	0.09	0.09	5205	417
5/27/24	62.8	65.3	35.5	30.3	0.07	0.08	4711	432
5/28/24	62.0	64.6	34.0	29.9	0.75	0.15	4140	311
5/29/24	63.9	61.3	35.2	29.9	0.08	0.13	3860	310
5/30/24	63.4	55.8	35.2	29.0	0.07	0.57	3387	87
5/31/24	63.0	52.1	35.0	27.8	0.53	0.32	3230	162
6/1/24	63.9	56.0	34.6	26.0	0.42	3.00	3025	288
6/2/24	63.7	65.4	35.7	29.4	0.43	0.20	2623	424
6/3/24	63.3	66.1	34.9	29.7	0.13	0.14	2056	440
6/4/24	63.2	66.7	35.2	29.8	0.09	0.15	1865	397
6/5/24	63.1	66.4	35.3	30.0	0.13	0.11	1673	373

6/6/24	63.1		33.9		0.35		1508	
6/7/24	64.2	59.0	34.3	28.9	0.27	0.60	1404	102

Table S10. Methane Yield from TS destruction

Date	CB	EB	CB		EB	
	L_{CH4}/day	L_{CH4}/day	$g_{TSremoved}$/day	$L_{CH4}/g_{TSremoved}$	$g_{TSremoved}$/day	$L_{CH4}/g_{TSremoved}$
5/19/23	1.33	1.28	1.62	0.82	1.66	0.77
5/23/23		1.33	1.42		1.46	0.91
5/26/23	1.12	1.30	1.89	0.60	1.94	0.67
6/2/23	1.12	1.19	1.72	0.65	1.78	0.66
6/6/23		1.20	1.48		1.49	0.81
6/9/23	0.98	1.15	1.74	0.56	1.75	0.65
6/13/23		1.18	1.48		1.41	0.83
6/16/23	0.89	1.12	1.63	0.55	1.62	0.69
6/20/23		1.29	1.48		1.46	0.88
6/23/23		1.16	1.75		1.77	0.66
6/27/23	1.12	0.92	1.44	0.78	1.46	0.63
6/30/23	1.04	1.21	1.74	0.60	1.74	0.70
7/7/23		1.19	1.35		1.48	0.81
7/11/23	1.02	1.26	1.30	0.78	1.43	0.88
7/14/23	1.26	1.49	1.10	1.15	1.25	1.20
7/18/23	1.04	1.15	0.97	1.08	1.15	1.00
7/21/23	1.07	1.15	1.28	0.84	1.42	0.81
7/25/23		1.11	1.03	0.00	1.22	0.91
8/1/23	1.02	1.20	1.24	0.82	1.36	0.88
8/4/23	0.87	0.94	1.34	0.65	1.58	0.59
8/8/23		1.75	1.13		1.43	1.22
8/14/23	0.36	0.88	1.34	0.27	1.62	0.54
8/18/23		1.04	1.31		1.62	0.64
8/25/23		1.01	1.07		1.36	0.74
8/29/23	0.94	1.33	0.82	1.15	1.12	1.19
9/1/23	0.13	0.80	1.34	0.09	1.67	0.48
9/5/23		0.78	0.94		1.29	0.61
9/8/23		0.81	1.40		1.65	0.49
9/12/23	1.11	1.12	1.36	0.81	1.62	0.69
9/15/23	1.00	0.09	1.45	0.69	1.70	0.05
9/19/23	1.02	1.35	1.32	0.78	1.62	0.84
9/22/23	0.99	0.47	1.19	0.83	1.36	0.34
9/26/23		1.17	0.47		0.72	1.63
10/6/23		0.03	1.73		1.70	0.02
10/17/23	1.08	0.30	1.47	0.73	2.14	0.14

10/20/23	1.16	0.96	1.56	0.74	2.17	0.44
10/24/23	1.15	1.20	1.58	0.73	2.01	0.60
10/27/23	1.01	0.57	1.50	0.67	1.88	0.30
10/31/23	1.02	1.48	1.59	0.64	1.78	0.83
11/3/23		0.86	1.50		1.82	0.47
11/7/23	0.19	1.17	1.51	0.13	1.63	0.72
11/10/23	0.82	1.12	1.61	0.51	1.62	0.70
11/14/23	0.83	1.22	1.86	0.45	1.90	0.64
11/17/23		0.88	1.28		1.23	0.71
11/21/23	0.18	1.28	1.55	0.12	1.50	0.86
11/24/23	0.81	0.90	1.46	0.55	1.41	0.64
11/28/23	0.72	0.97	1.59	0.45	1.51	0.64
12/1/23		0.95	1.43		1.45	0.65
12/5/23	0.57	0.87	1.42	0.39	1.46	0.60
12/8/23		1.37	1.66		1.66	0.83
1/4/24	0.24	1.22	1.49	0.16	1.53	0.80
1/9/24	0.85	1.22	1.57	0.54	1.69	0.72
1/15/24		1.31	1.70		1.82	0.72
1/19/24	1.03	1.18	1.52	0.68	1.68	0.70
1/22/24	1.25	1.63	1.53	0.82	1.64	1.00
1/29/24	0.86	0.63	1.82	0.47	1.86	0.34
2/2/24	0.87	1.08	1.54	0.56	1.66	0.65
2/6/24		0.87	1.76		1.78	0.49
2/9/24	1.22	1.59	1.82	0.67	1.98	0.80
2/13/24		1.18	1.62		1.66	0.71
2/16/24	1.06	1.21	1.15	0.92	1.38	0.87
2/20/24	0.96	1.14	1.48	0.65	1.63	0.70
2/23/24	0.80	1.19	1.37	0.59	1.54	0.78
2/26/24	0.56	1.30	1.54	0.36	1.71	0.76
2/29/24		0.89	1.20		1.37	0.65
3/4/24	1.59	1.33	1.52	1.05	1.66	0.80
3/11/24	0.56	1.24	1.42	0.39	1.54	0.81
3/14/24	0.58	1.21	1.75	0.32	1.90	0.64
3/18/24	0.61	1.41	1.65	0.37	1.74	0.81
3/24/24	0.74	0.72	1.35	0.55	1.42	0.51
3/28/24	1.20	0.92	1.41	0.86	1.66	0.56
4/2/24	1.64	0.88	1.68	0.97	1.90	0.46
4/5/24	1.56	1.59	1.62	0.97	1.85	0.86

4/8/24	0.94	1.21	1.43	0.66	1.67	0.72
4/12/24	1.05	0.80	1.39	0.76	1.76	0.46
4/15/24	0.90	1.25	1.42	0.63	1.66	0.75
4/18/24	1.28	1.49	1.38	0.93	1.46	1.02
4/22/24	0.92	1.49	1.68	0.55	1.74	0.86
4/25/24	0.90	1.44	1.36	0.66	1.42	1.02
4/29/24	0.89	1.41	1.47	0.60	1.47	0.96
5/2/24	0.89	1.36	1.51	0.59	1.50	0.90
5/6/24	1.30	0.79	1.54	0.84	1.54	0.51
5/9/24	1.16	1.29	1.56	0.74	1.50	0.86
5/13/24	0.93	1.24	1.82	0.51	1.62	0.77
5/20/24	0.72	1.62	0.96	0.75	1.68	0.97
5/23/24	1.53	1.30	1.02	1.50	1.58	0.83
5/27/24	1.53	1.31	1.54	1.00	1.97	0.67
5/30/24	0.48	1.13	1.26	0.38	1.68	0.67
6/3/24	1.24	1.22	1.70	0.73	1.75	0.69
6/7/24	0.52	1.69	1.74	0.30	1.74	0.97

Table S11. Total Sulfur concentrations measured in the feed and the effluents of EB and CB.

Date	Feed	EB	CB
	mg/L	mg/L	mg/L
10/31/23	377	296	354
11/3/23	378	301	342
11/7/23	401	342	345
11/10/23	374	348	338
11/14/23	386	354	354
11/17/23	342	352	334
11/21/23	362	348	332
11/24/23	355	336	327
11/28/23	382	336	327
12/1/23	354	329	341
12/5/23	341	316	318
12/8/23	378	322	327
12/12/23	382	321	333
12/15/23	395	318	333
12/19/23	397	324	357
12/22/23	389	328	360
12/27/23	417	332	340
12/28/23	402	336	345
1/4/24	385	325	347
1/5/24	407	332	346
1/9/24	403	327	346
1/15/24	395	331	358
1/19/24	376	324	333
1/22/24	364	311	343
1/29/24	396	311	333
2/2/24	363	297	336
2/6/24	361	330	324
2/9/24	346	314	334
2/13/24	386	320	332
2/16/24	342	298	335
2/20/24	372	310	334
2/23/24	350	286	335
2/26/24	393	306	333
2/29/24	349	298	321
3/4/24	365	301	332

3/7/24	338	288	327
3/11/24	348	281	299
3/14/24	368	278	308
3/18/24	360	299	321
3/24/24	346	305	314
3/25/24	333	295	309
3/28/24	339	279	321
4/2/24	380	297	307
4/5/24	369	285	319
4/8/24	330	279	307
4/12/24	333	269	319
4/15/24	348	264	330
4/18/24	342	296	312
4/22/24	347	311	314
4/25/24	332	307	306
4/29/24	346	325	326
5/2/24	362	328	316
5/6/24	344	302	304
5/9/24	380	324	314
5/13/24	393	330	317
5/17/24		307	356
5/20/24	370	315	492
5/23/24	364	305	468
5/27/24	408	298	421
5/30/24	390	297	411
6/3/24	399	312	369
6/7/24	388	311	345

REFERENCES

Almansa, X.F., Starostka, R., Raskin, L., Zeeman, G., De Los Reyes, F., Waechter, J., Yeh, D. and Radu, T. 2023. Anaerobic Digestion as a Core Technology in Addressing the Global Sanitation Crisis: Challenges and Opportunities. Environmental Science & Technology 57(48), 19078-19087.

American Public Health Association, A.W.W.A., and Water Environment Federation (1997) Standard Methods For the Examination of Water and Wastewater. Lipps, W.C., Baxter, T.E. and Braun-Howland, E. (eds), APHA Press, Washington DC.

Azizi, S.M.M., Zakaria, B.S., Haffiez, N., Niknejad, P., Maal-Bared, R., Molla, S. and Dhar, B.R. 2023. Bench-Scale Liquid-Phase Microaeration and Iron Dosing Comparison for In Situ Biogas Desulfurization and Antibiotic Resistance Management in Mesophilic Anaerobic Digestion. ACS ES&T Water 3(8), 2458-2470.

Chen, Q., Wu, W., Qi, D., Ding, Y. and Zhao, Z. 2020. Review on microaeration-based anaerobic digestion: State of the art, challenges, and prospectives. Science of The Total Environment 710.

do Nascimento, J.G.d.S., Silva, E.V.A., dos Santos, A.B., da Silva, M.E.R. and Firmino, P.I.M. 2021. Microaeration improves the removal/biotransformation of organic micropollutants in anaerobic wastewater treatment systems. Environmental Research 198.

EPA, U. 1996 SW–846. Response, E.O.o.S.W.a.E. (ed).

EPA, U.S. 1994 Method 200.7: Determination of Metals and Trace Elements in Water and Wastes by Inductively Coupled Plasma-Atomic Emission Spectrometry, Revision 4.4. Agency, U.S.E.P. (ed).

Fu, S., Lian, S., Angelidaki, I. and Guo, R. 2023. Micro-aeration: an attractive strategy to facilitate anaerobic digestion. Trends in Biotechnology 41(5), 714-726.

Giordano, A., Di Capua, F., Esposito, G. and Pirozzi, F. 2019. Long-term biogas desulfurization under different microaerobic conditions in full-scale thermophilic digesters co-digesting high-solid sewage sludge. International Biodeterioration & Biodegradation 142, 131-136.

Hoque, A. and Paul, A.K. 2022. Experimental investigation of oxygen transfer efficiency in hydraulic jumps, plunging jets, and plunging breaking waves. Water Supply 22(4), 4320-4333.

IEA 2018 The energy sector should care about wastewater, IEA, Paris.

Ingle, A.T., Fortney, N.W., Walters, K.A., Donohue, T.J. and Noguera, D.R. 2021. Mixed Acid Fermentation of Carbohydrate-Rich Dairy Manure Hydrolysate. Frontiers in Bioengineering and Biotechnology 9.

Khanal, S.K. 2008. Microbiology and biochemistry of anaerobic biotechnology. Anaerobic biotechnology for bioenergy production: principles and applications, 29-41.

Krayzelova, L., Bartacek, J., Díaz, I., Jeison, D., Volcke, E.I.P. and Jenicek, P. 2015. Microaeration for hydrogen sulfide removal during anaerobic treatment: a review. Reviews in Environmental Science and Bio/Technology 14(4), 703-725.

Li, R., Guo, X., Xiong, K., Xing, X. and Zhang, C. 2023. Microbial micro-tube culture system: A miniature bioreactor for controllable bubble-free oxygen supply based on high gas-permeability Teflon tube. Biochemical Engineering Journal 191.

Nguyen, D. and Khanal, S.K. 2018. A little breath of fresh air into an anaerobic system: How microaeration facilitates anaerobic digestion process. Biotechnology Advances 36(7), 1971-1983.

Nguyen, D., Wu, Z., Shrestha, S., Lee, P.-H., Raskin, L. and Khanal, S.K. 2019. Intermittent micro-aeration: New strategy to control volatile fatty acid accumulation in high organic loading anaerobic digestion. Water Research 166.

Ortiz-Ardila, A.E., Celis, C., Usack, J.G., Angenent, L.T. and Labatut, R.A. 2024. Microaeration promotes volatile siloxanes conversion to methane and simpler monomeric products. Bioresource Technology 400.

Oude Elferink, S.J.W.H., Visser, A., Hulshoff Pol, L.W. and Stams, A.J.M. 1994. Sulfate reduction in methanogenic bioreactors. FEMS Microbiology Reviews 15(2-3), 119-136.

Pokorna-Krayzelova, L., Vejmelkova, D., Selan, L., Jenicek, P., Volcke, E.I.P. and Bartacek, J. 2018. Final products and kinetics of biochemical and chemical sulfide oxidation under microaerobic conditions. Water Sci Technol 78(9), 1916-1924.

Rasi, S., Läntelä, J. and Rintala, J. 2011. Trace compounds affecting biogas energy utilisation – A review. Energy Conversion and Management 52(12), 3369-3375.

Roosta, A., Jahanmiri, A., Mowla, D. and Niazi, A. 2011. Mathematical modeling of biological sulfide removal in a fed batch bioreactor. Biochemical Engineering Journal 58-59, 50-56.

Sanderson, K. 2023 COP28 climate summit signals the end of fossil fuels — but is it enough?, pp. 484-485.

Smith, R., Elger, S. and Mleziva, S. 2018 Solids Retention Time Control in Water Resource Recovery Facilities.

Tang, Y., Shigematsu, T., Ikbal, Morimura, S. and Kida, K. 2004. The effects of micro-aeration on the phylogenetic diversity of microorganisms in a thermophilic anaerobic municipal solid-waste digester. Water Research 38(10), 2537-2550.

Tessele, F. and van Lier, J. 2020. Anaerobic digestion and the circular economy. Water e-Journal 5(3), 1-5.

Vu, H.P., Nguyen, L.N., Wang, Q., Ngo, H.H., Liu, Q., Zhang, X. and Nghiem, L.D. 2022. Hydrogen sulphide management in anaerobic digestion: A critical review on input control, process regulation, and post-treatment. Bioresource Technology 346.

Wei, C.-H., Wang, Z.-W., Dai, J.-H., Xiao, K., Yu, H.-R., Qu, F.-S., Rong, H.-W., He, J.-G. and Ngo, H.H. 2024. Enhanced anaerobic digestion performance and sludge filterability by membrane microaeration for anaerobic membrane bioreactor application. Bioresource Technology 402.

Xu, S., Selvam, A. and Wong, J.W.C. 2014. Optimization of micro-aeration intensity in acidogenic reactor of a two-phase anaerobic digester treating food waste. Waste Management 34(2), 363-369.